



# Net zero roadmap modelling for sustainable dairy manufacturing and distribution

Maria Ioanna Malliaroudaki<sup>a</sup>, Nicholas J. Watson<sup>a</sup>, Zachary J. Glover<sup>b</sup>, Luanga N. Nchari<sup>c</sup>, Rachel L. Gomes<sup>a,\*</sup>

<sup>a</sup> Food Water Waste Research Group, Faculty of Engineering, University of Nottingham, Nottinghamshire NG7 2RD, United Kingdom

<sup>b</sup> Arla Foods Ltd., Arla House, Leeds LS10 1AB, United Kingdom

<sup>c</sup> NIZO, Kernhemseweg 2, Ede 6718 ZB, the Netherlands

## ARTICLE INFO

### Keywords:

Energy  
Carbon footprint  
Pasteurisation  
Decarbonisation  
Supply chain  
Dairy manufacturing

## ABSTRACT

Energy-derived carbon emissions from dairy manufacturing and distribution are significant. Meeting a net zero carbon target is a global priority, and to that end the dairy industry is engaging an emission-reduction strategy. Modelling tools that can predict energy consumption and related carbon-emissions can aid decision-making towards energy transitioning. This study presents an energy consumption model for dairy skimmed milk and cream manufacturing and distribution, which has been developed following a mechanistic modelling approach. This approach integrates chemical engineering process design, heat exchange principles, and empirical modelling to simulate energy consumption for each individual supply chain component, sequence-by-sequence. The model offers simulation flexibility, allowing the projection of the product's embodied energy and carbon-emissions under diverse manufacturing and distribution scenarios. To investigate the model capabilities, scenario analysis was performed for 12 different scenarios. These scenarios resulted by testing the use of three fuel types for the heating requirements in manufacturing (oil, natural gas and hydrogen), two categories of refrigerated vehicles (diesel and electric), and two different distribution infrastructures (centralised and decentralised). The evaluated skimmed milk product-embodied energy ranged between 309 and 869 kJ/L. The scenarios were also simulated towards 2050 using the UK projections for electricity's carbon conversion factor to predict the anticipated carbon-emission reductions. These 2050 projections allowed for roadmap planning towards decarbonising energy for skimmed milk and cream manufacturing and distribution, with outcomes demonstrating up to 90.2% carbon-emission reductions by 2050. The developed model can support safe decision-making and assist the dairy industry in meeting the net zero carbon target.

## 1. Introduction

Society is currently approaching a tipping point in the battle to mitigate global warming. A detailed understanding of energy-related carbon emissions is required to enable impactful decision-making in industry, both at national, and international levels. The food sector accounts for approximately 30% of global energy consumption [1,2], while food manufacturing and distribution are responsible for >38% of the global food sector's energy consumption [3]. The dairy industry has demanding energy requirements in process manufacturing due to intensive heating and cooling needs and in product distribution due to

refrigeration and transportation requirements [4]. In addition, the global consumption of dairy products where cheese, milk, and butter comprise ~14% and ~5% of the total dietary intake in high and low to middle income countries respectively, will make any improvements in the sector's sustainability significantly impactful [5]. Moreover, a carefully devised strategy to mitigate energy consumption in the dairy sector can inspire the wider food and drink industry, since a significant portion of operations within the food and drink industry are grounded in the activities of the dairy sector [6].

Energy consumption within the dairy sector is expected to rise due to global warming and population growth [7]. The increasing ambient

**Abbreviations:** GHG, greenhouse gas; MM, Mechanistic model; LCA, Life Cycle Assessment; COP, Coefficients of performance; PHE, Plate heat exchanger; CIP, Cleaning-in-place; DC, Direct currency; CO<sub>2</sub>e, Carbon dioxide equivalent emissions; TRL, Technology readiness level.

\* Corresponding author.

E-mail address: [rachel.gomes@nottingham.ac.uk](mailto:rachel.gomes@nottingham.ac.uk) (R.L. Gomes).

<https://doi.org/10.1016/j.cej.2023.145734>

Received 27 June 2023; Received in revised form 25 August 2023; Accepted 28 August 2023

Available online 1 September 2023

1385-8947/© 2023 The Authors. Published by Elsevier B.V. This is an open access article under the CC BY license (<http://creativecommons.org/licenses/by/4.0/>).

temperatures and the more frequent heatwave events in many parts of the world will set the requirement of lowering the refrigeration temperatures to ensure food security. The lower refrigeration temperatures and the higher gradient between refrigeration and ambient temperature during the hot days, will pose an additional energy load to the dairy supply chain [8]. In parallel, world population growth will drive an estimated >60% increase in the demand for dairy products by 2050, versus 2000 levels [9]. An energy mitigation strategy spanning the entire dairy sector (from “farm-to-fork”) should be developed to support the reduction of energy-derived emissions responsible for global warming, whilst still being able to meet the food demand of growing populations. Along the dairy supply chain, product manufacturing and distribution together are responsible for the lion’s share of the energy-derived carbon emissions. For example, in the milk supply chain, manufacturing and distribution is estimated to be responsible for around 45% of total energy-derived greenhouse gas (GHG) emissions produced along the “farm-to-fork” supply chain [10,11]. Therefore, there is an urgent need to focus on mitigating energy use of those interdependent supply chain stages [10].

Governments around the globe have set their own sustainability targets to meet net zero carbon levels by 2050, as per the Paris Agreement [12], “Net zero carbon” means that the anthropogenic carbon emissions that cross the boundaries of a system should be balanced by the anthropogenic carbon emission removals through those boundaries [13]. As part of net zero carbon target, the European Union aims for a 55% reduction in overall carbon emissions by 2030 [14]. The report by Ricardo Energy & Environment on behalf of FoodDrinkEurope investigates and recommends decarbonisation pathways for the European food and drink manufacturing sector [15]. Focusing on the energy mitigation targets for UK dairy manufacturers, over 90 dairies across 60 companies have committed to achieve 30% relative reductions in carbon emissions related to energy use at their processing sites by 2025, compared to 2008 levels [16]. The food and drink industry are under pressure to take actions driven by a number of national, international and self-imposed targets. Some of the key strategies to support decarbonisation will focus on shifting to renewable energy and transforming the production system towards centralised or decentralised production, depending on financial and environmental benefits.

For the year 2023, food and dairy manufacturing is still predominantly dependent on fossil fuels. A complete fossil fuel phase-out is required to reach the net zero carbon target by 2050 [17]. Under this energy transition, the industrial and transportation sectors aim to move towards process electrification and greener fuels such as hydrogen. Process electrification is when processes are converted from a fuelled-powered to an electric-powered technology. Process electrification can lead to a gradual process decarbonisation, benefiting from the national or regional grid decarbonisation, in line with the net zero carbon target [18]. Process electrification can also lead to complete process decarbonisation when renewable energy is used directly to power the process [19]. Regarding the electrification of transportation, although fully electric refrigerated vehicles have not been currently released at scale, electric transportation is expected to be the dominant form of logistics in the future [20].

Hydrogen is a zero-carbon fuel since its combustion produces water and is currently considered a likely fuel alternative for the future across many industrial sectors [21]. Although hydrogen combustion has zero carbon emissions, the use of hydrogen may still have a carbon impact, depending on the primary production technology utilised [22]. A complete net zero hydrogen production technology is via water electrolysis powered by renewable energy, such as solar or wind. This is often called “green hydrogen” because its production causes the release of minimal or zero GHG emissions [23]. Hydrogen can also be produced from natural gas via steam methane reforming [23]. This technology generates significant carbon emissions and therefore is called “grey hydrogen”. When carbon capturing technologies are used in steam methane reforming, this leads to reduced net carbon emissions. Hydrogen

produced through this technology is called “blue hydrogen”, and is more environmental friendly compared to grey hydrogen [23]. However, both blue and grey hydrogen have a carbon footprint [20].

The future sustainability of the food and dairy sector does not only rely on energy transitioning but also on the future size and shape of product distribution infrastructure. One consideration is whether it would be more environmentally and financially sustainable if the future dairy sector is transformed towards a more centralised or a decentralised product distribution infrastructure [22,24]. Existing large-scale centralised food production has significant freight transportation needs, accompanied by corresponding significant levels of energy use and emissions [22]. However, large scale production tends to require less energy and cost per unit of product due to the economy of scale [25,26]. Two noteworthy examples of intense centralised production are a mega dairy farm located in China, which is home to almost 100,000 cows [27] and a high-technology dairy processing plant located in the UK that processes up to 240,000 L per hour, providing 10% of the milk supply for the UK [28]. In contrast, decentralised dairy production has lower transportation energy needs. However, production at the smaller scale may require higher energy and cost demand per unit, compared to large scale production [29].

Any energy mitigation actions for the dairy supply chain must be made through a well-planned strategy. Models can provide a holistic measurement of energy use and interactions between the supply chain stages which significantly contribute to energy and emissions mitigation planning [30,10]. As a result, reliable energy consumption models should be developed to aid decision-making. Such models will be able to identify the most energy consuming operations, whilst simulating future scenarios of the dairy supply chain and evaluating the potential energy savings through alternative processes and scenarios [10,31,32].

Studies in the field of food systems’ modelling traditionally focus on improving product quality and reducing cost. In the past decade to 2023, there has been growing research interest in modelling food systems to also manage environmental impacts [33]. This is due to a growing appreciation that such impacts carry a cost that can continually increase over time (e.g. waste management), as well as regulatory or legislative environmental drivers. A number of studies have modelled dairy manufacturing using a process design approach to estimate the total manufacturing energy use under different production scenarios [34,35]. Other studies performed multi-objective optimisation for both environmental sustainability and economic performance of dairy products [36,37]. Several studies also assessed the future energy performance of dairy production by simulating potentially more sustainable scenarios in terms of energy mix and the specific combinations of different energy sources [38,39]. However, there is no existing work in the literature that offers a flexible model for food systems’ manufacturing and distribution that is capable of evaluating different scenarios and assessing for each scenario their energy and sustainability performance.

The development of a food system energy consumption model that mitigates energy use in dairy manufacturing and distribution would be potentially invaluable. Mechanistic models (MM) are mathematical models that apply first principles and empirical modelling to predict the mechanistic behaviour of a system [40]. Mechanistic models provide simulation flexibility due to the ability to test different scales of production and technologies. A mechanistic energy consumption model can be simulated under a range of production and supply scenarios to identify the least energy consuming and emitting scenarios. In addition, such models can be used for the strategic planning of a well-thought roadmap towards the net zero target [10]. Such models may also be integrated into Life Cycle Assessment (LCA) tools to enable the quantification of the total system’s environmental impact. Currently, modelling food systems’ energy consumption following a MM approach in the literature is sparse [34,35,40,41]. However, although an MM approach in food systems is not yet widely applied, it is highly recommended, since it offers the flexibility that can support decision making for continuously changing systems and develop an adaptive roadmap to

become net zero by 2050.

In the present study, a mechanistic energy consumption model was developed to evaluate the energy use and carbon footprint of dairy skimmed milk and cream products under 12 manufacturing and distribution scenarios. Moreover, the annual energy derived carbon emissions of skimmed milk and cream manufacturing and distribution under those scenarios were projected towards 2050, allowing the development of an energy transition roadmap that can be adaptive to changing energy options and industry drivers as they appear. The scope and impact of this paper can be scaled beyond the dairy sector to the broader food and drink industry, since the modelled processes and operations are replicated for many other food and drink product types. Whilst this work can inspire the development of similar models, for any industrial sector that aims to tackle emissions and energy use.

## 2. Materials and methods

This section presents the modelling methodology for the development of the energy consumption model for dairy skimmed milk and cream manufacturing and distribution. A mechanistic modelling approach was followed to provide simulation flexibility for different scales of production, processing conditions and energy resources used. This approach integrates chemical engineering process design, heat exchange principles, and empirical modelling, to simulate energy consumption for each individual supply chain component “sequence-by-sequence”. Specifically, the following stages were modelled (Fig. 1):

1. Raw milk reception and cold storage.
2. Skimmed milk and cream processing units.
3. Cleaning-in-place for the processing lines.
4. Packaging process.
5. Cold storage in chambers in the manufacturing plant.
6. Refrigerated transportation to the distribution centre.
7. Cold storage in chambers in the distribution centre.
8. Refrigerated transportation from the distribution centre to the retail outlet.

The energy consumption model was developed following the steps below. Each step corresponds to the respective [Sections 2.1-2.3](#):

To model the skimmed milk and cream processing units, standard chemical engineering process design methods and heat exchange principals were applied. This allowed the estimation of the utilities demand (steam, chilled water, cleaning fluids), to scale the equipment used and calculate the pressure states ([Section 2.1](#)).

To measure the thermal load on the refrigerated facilities along skimmed milk and cream manufacturing and distribution, heat exchange principals were applied. The equipment or facilities modelled following this approach were the cold storage of raw milk in reception, product storage in the manufacturing plant and distribution centre and the refrigerated unit of the refrigerated vehicles ([Section 2.2](#)).

Steps 1 and 2 allowed the evaluation of the total heating, cooling and pumping energy input required in product manufacturing and distribution. This energy is provided to the system through electrical and fuelled-powered equipment. To measure the electricity demand and fuel demand of those equipment, empirical models and coefficients of performance (COP) were used. In addition, the energy usage of mechanical processes such as packaging and transportation were evaluated through benchmarking values available in the literature ([Section 2.3](#)).

The model developed formulates a set of linear and non-linear algebraic equations, which were simultaneously solved through a programme developed in Microsoft Excel (version 2307), for a set of parameters that differ for each scenario simulated.

### 2.1. Modelling skimmed milk and cream processing units

The skimmed milk and cream processing unit modelled is illustrated in the flowchart (Fig. 2) and represents a conventional processing line. In this processing unit, whole milk stream is heated at 50–60 °C and pumped into a centrifugal separator, where the globular milk fat is

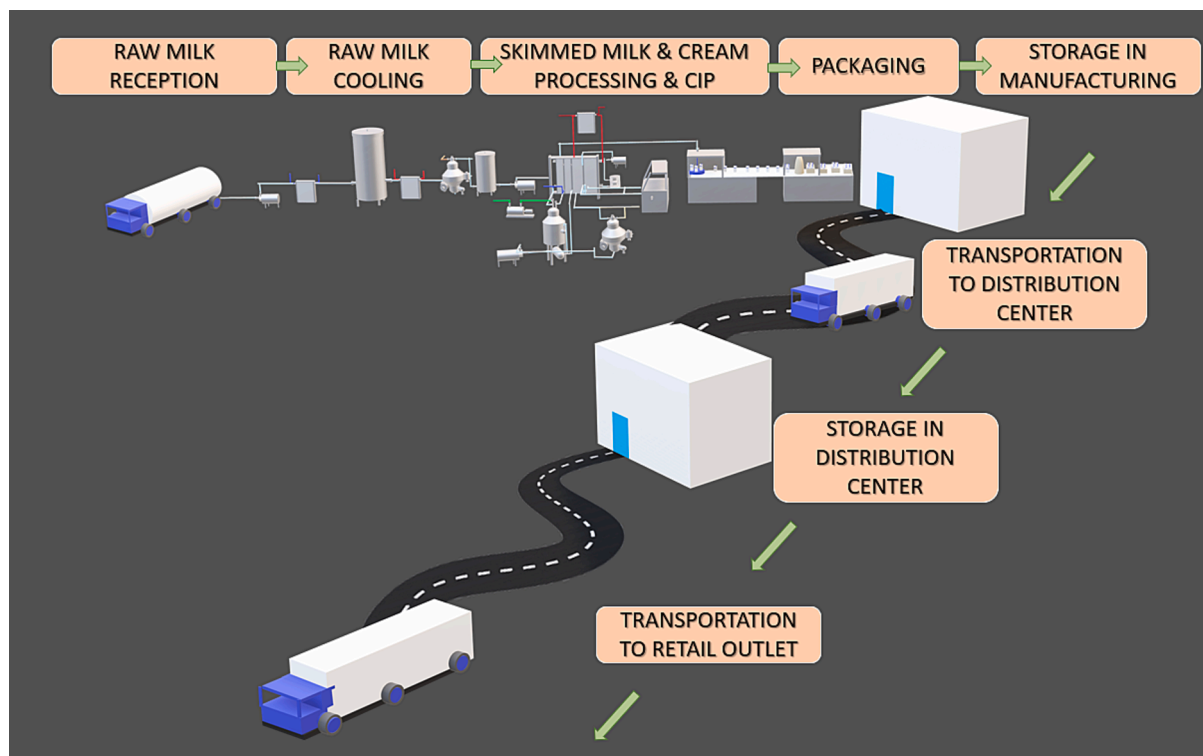
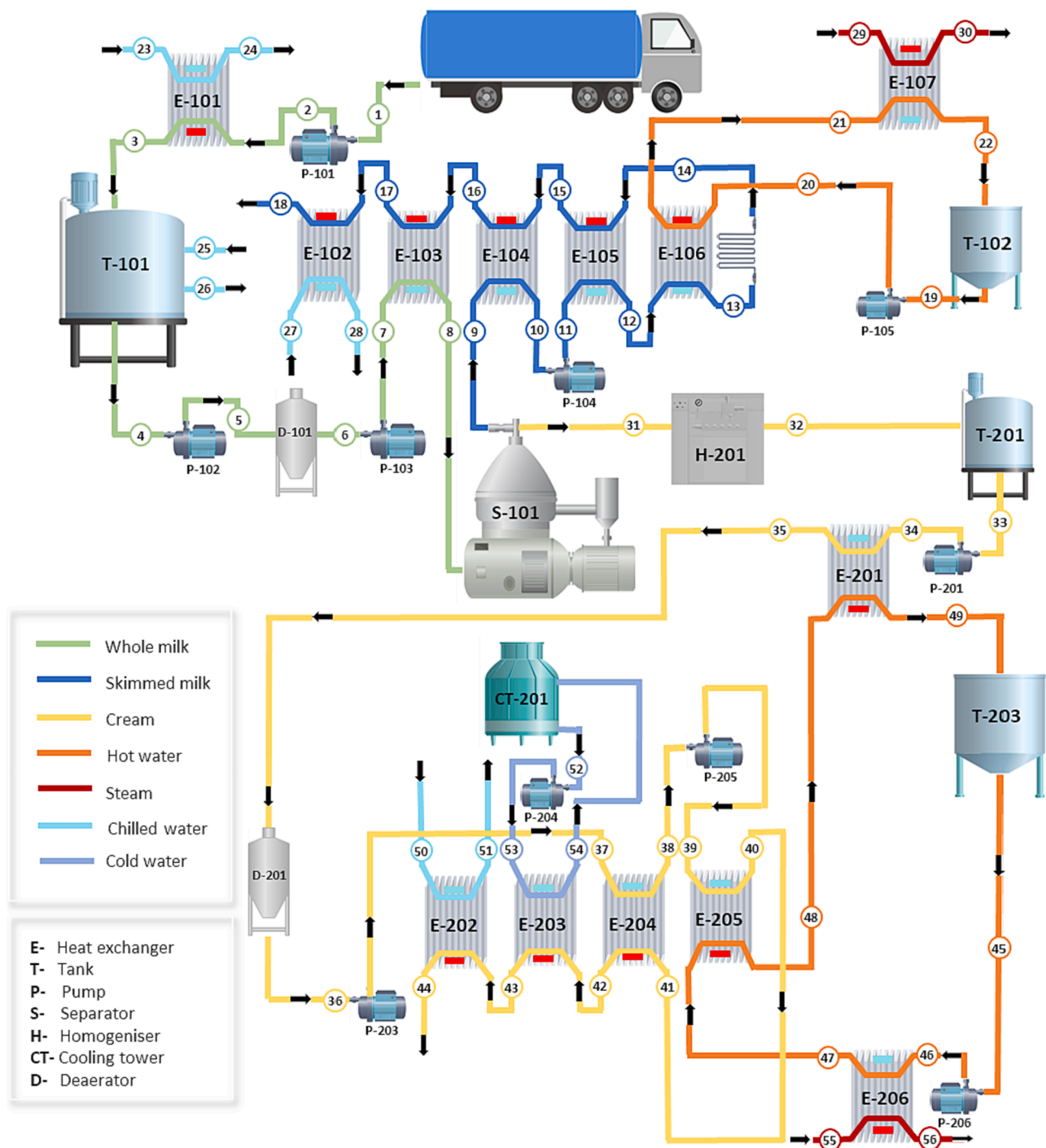


Fig. 1. Illustration of the modelled stages of skimmed milk and cream manufacturing and distribution.



**Fig. 2.** Flow chart illustration of a skimmed milk and cream processing unit, where raw whole milk is preheated and separated in a skimmed milk and a cream stream, which are then pasteurised and cooled down in the skimmed milk processing lines (above) and the cream processing line (below) respectively. Streamline colours and equipment symbols are explained in the left side of the flowchart. The flowchart is adapted from the study of Singh et al., (2020) [43].

separated from the serum. This process leads to two output streams each having a different fat content, a stream of cream and a stream of skimmed milk. These streams are then pasteurised and then quickly cooled down, after which the pasteurised streams are passed to the packaging units [42].

The flowchart of Fig. 2 is adapted from the study of Singh et al., (2020) [43]. As illustrated, the raw milk produced at farms arrives at the dairy processing via refrigerated vehicles, which maintain the milk at a temperature of  $\sim 5^{\circ}\text{C}$ . The raw milk is then pumped from the truck through the heat exchanger E-101 where the milk is cooled to  $4^{\circ}\text{C}$  via

the chilled water supply to the cooling tank T-101. When production begins, the milk is pumped to the milk balance tank D-101 for deaeration. Then enters the centrifugal separator S-101 after being preheated to  $54^{\circ}\text{C}$  through the heat exchanger E-103 in order to be separated more effectively [44]. Through the separation process, stream 8, is separated into a skimmed milk stream (stream 9) and a cream stream (stream 31). Stream 9 leads to the skimmed milk processing unit, while stream 31 is homogenised through H-201 and then leads to the cream processing unit.

In the orange colour streamline (streams 19–22) of the skimmed milk

processing unit in Fig. 2, hot water recirculates to deliver the required heat for milk pasteurisation. Heat is provided to the hot water recirculating system via the steam supply (stream 29) to the heat exchanger E-107, where stream 21 enters the E-107 and the water is heated up to 85 °C (stream 22). Milk pasteurisation is achieved by heating the milk to 72–76 °C and is required to remain at this temperature for 15 s and for that purpose a coil tube is used [43]. After pasteurisation, the milk needs to cool down quickly. The cooling process of milk begins in the heat exchanger E-105 and continues to the heat exchangers E-104 and E-103 through regenerative heating, by capitalising on the cooler milk streams. Finally, in the heat exchanger E-102, chilled water is provided at 1 °C to cool down the pasteurised milk to 3.5 °C, ready to be packaged.

A similar process occurs in the cream processing unit where cream pasteurisation is achieved by raising the temperature of cream to 88 °C for 1 s before immediately cooling it down to 7 °C. The homogenised cream of stream 32 is pumped through heat exchanger E-201 where it is heated up by the hot water supply (stream 48) of the cream processing unit, to balance any heat losses that occur if cream is temporarily stored in tank T-201. The cream then passes through the deaerator device D-201 to the cream pasteuriser. In the heat exchanger E-205 cream reaches its highest temperature of 88 °C via hot water supply (stream 53). Finally, the heat exchanger E-203 cools down the cream through a cooling tower system (CT-201), and further cooling is achieved in the heat exchanger E-202 via chilled water supply (stream 50). These both cool the pasteurised cream to 7 °C, ready to be packaged.

### 2.1.1. Material properties for modelling the product processing units

Material property values were required to resolve the mass and energy balance equations as well as for the heat exchangers' design (Section 2.1.2), the pipeline diameter selection (Section 2.1.3), the energy demand for the cleaning-in-place process (Section 2.1.4) and for the pressure drop estimation (Section 2.1.5). These properties were the density  $\rho$ , the specific heat capacity  $C_p$  and the dynamic viscosity  $\mu$ . Empirical models for the aforementioned properties for milk, cream, water and steam are provided in Section A of the [Supplementary Material](#).

### 2.1.2. Mass and energy balances

To determine the flow rate and temperature for each stream of the flowchart in Fig. 2, a standard chemical engineering process design approach was followed [38]. For each process taking place through the processing line (e.g. heat exchange, separation, homogenisation), a unit operation was considered. The mass and energy balances for each unit operation were resolved accounting for the input and output flow streams [45].

The mass balance equation for a unit operation in the Fig. 2 flowchart under steady state, where no chemical reactions are taking place and there is no mass accumulation, may be written as follows:

$$\sum_i \dot{m}_{i,in} = \sum_j \dot{m}_{j,out} \quad (1)$$

Where,  $\dot{m}_{i,in}$  and  $\dot{m}_{j,out}$  are the mass flow rates of the inlet and outlet stream  $i$  to the unit operation.

The general energy balance for a unit operation under steady state respectively, given that no chemical reactions occur and if energy losses and energy input due to mechanical work are neglected, may be written as follows:

$$\sum_i \dot{H}_{i,in} + \dot{Q}_{net,in} - \dot{W}_{net,out} = \sum_j \dot{H}_{j,out} \quad (2)$$

Or,

$$\sum_i h_{i,in} \dot{m}_{i,in} + \dot{Q}_{net,in} - \dot{W}_{net,out} = \sum_j h_{j,out} \dot{m}_{j,out} \quad (3)$$

Where,  $\dot{Q}_{net,in}$  is the net heat rate input to the system,  $\dot{W}_{net,out}$  is the net

work rate output from system,  $\dot{H}_{i,in}$  is enthalpy rate of the inlet stream  $i$  and  $\dot{H}_{j,out}$  is the enthalpy rate of the outlet stream  $j$  of a unit operation respectively and  $h_{i,in}$  and  $h_{j,out}$  are the specific enthalpy of the inlet and outlet streams respectively.

**2.1.2.1. Mass balance for the separation process.** In the separation process taking place in the centrifugal separator (S-101), the inlet stream 8 is separated into stream 9 of skimmed milk (low fat stream) and stream 31 of cream (rich in fat stream). Due this composition difference between the streams, the mass balance equation for the fat substance (Eq. (6)) should be considered alongside the total material mass balance (Eq. (7)) in the calculations:

Total material mass balance for the separator S-101:

$$\dot{m}_{wm,in} = \dot{m}_{sm,out} + \dot{m}_{c,out} \quad (4)$$

Where,  $\dot{m}_{wm,in}$  is mass flow rate of whole milk stream entering the separator and  $\dot{m}_{sm,out}$  and  $\dot{m}_{c,out}$  are the mass flow rates of the skimmed milk and cream outlet streams of the separator respectively.

Fat substance mass balance for the separator S-101:

$$F_{wm,in} \dot{m}_{wm,in} = F_{sm,out} \dot{m}_{sm,out} + F_{c,out} \dot{m}_{c,out} \quad (5)$$

Where,  $F_{wm,in}$ ,  $F_{sm,out}$ , and  $F_{c,out}$  is the fat content (w/w %) of each stream entering or exiting the separator.

**2.1.2.2. Mass & energy balance in heat exchangers.** The most commonly used heat exchangers in the dairy industry are plate heat exchangers (PHEs) since they offer a large heat exchange surface in a compact structure and have a low fouling factor, which means that they can be cleaned relatively easy [46]. PHEs consist of closely spaced thin plates held tightly together in a gasket frame [47]. Fig. 3 illustrates the phenomena occurring in a counter flow plate heat exchanger, showing the pathways of the hot and cold streams. Fig. 4 represents a simplified illustration of a PHE that corresponds to PHE representations used in the flowchart of Fig. 2.

The difference of the specific enthalpy between the inlet and the outlet of a stream passing through a heat exchanger  $\Delta h$ , in low pressures with no phase change, was calculated by Eq. (6):

$$\Delta h = h_{out} - h_{in} = \int_{T_{in}}^{T_{out}} C_p dT \quad (6)$$

While if there is phase change, Eq. (7) can be applied, where + is used when the phase change is evaporation and – if the phase state is condensation.

$$\Delta h = h_{out} - h_{in} = \pm \Delta h_{vap} + \int_{T_{in}}^{T_{out}} C_p dT \quad (7)$$

Where,  $T_{in}$  and  $T_{out}$  are the inlet and outlet temperature of the stream in one side of the heat exchanger,  $C_p$  is the specific heat capacity at constant pressure and  $\Delta h_{vap}$  is the latent heat of vaporization.

Therefore, for a counter flow heat exchanger, the mass and energy balance equation results from applying Eq. (6) or (7) to the general mass and energy balance equations (Eqs. (1) and (3)), given by Eq. (8):

$$\dot{m}_c \int_{T_{c,in}}^{T_{c,out}} C_{p,c} dT \left( + \dot{m}_c \Delta h_{vap,c} \right) = - \dot{m}_h \int_{T_{h,in}}^{T_{h,out}} C_{p,h} dT \left( + \dot{m}_h \Delta h_{vap,h} \right) \quad (8)$$

Where,  $\dot{m}_h$ ,  $T_{h,in}$  and  $T_{h,out}$  are the mass flowrate, the inlet and the outlet temperature of the hot side stream, and  $\dot{m}_c$ ,  $T_{c,in}$  and  $T_{c,out}$  are the mass flowrate, the inlet and the outlet temperature of the cold side stream respectively (as shown in Figs. 3 and 4). Empirical models for the specific heat capacities of the hot and cold side streams,  $C_{p,h}$  and  $C_{p,c}$ , are provided in Section A of the [Supplementary Material](#).

A simplistic and convenient design method was used to size the heat exchangers [47]. The first step was to estimate the duty exchange rate between the hot and the cold stream side of each heat

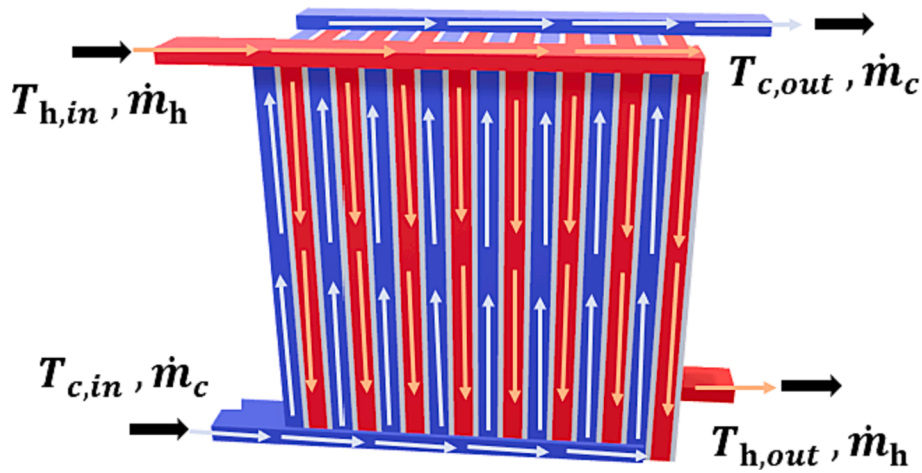


**Fig. 3.** Schematic representation of a counter-flow Plate Heat Exchanger. The blue stream represents the cold side stream while the red stream represents the hot side stream. Where,  $\dot{m}$ ,  $T_{in}$  and  $T_{out}$  are the mass flowrate, the inlet and the outlet temperature of the stream in one the cold (c) or hot (h) side of the heat exchanger. (For interpretation of the references to colour in this figure legend, the reader is referred to the web version of this article.)

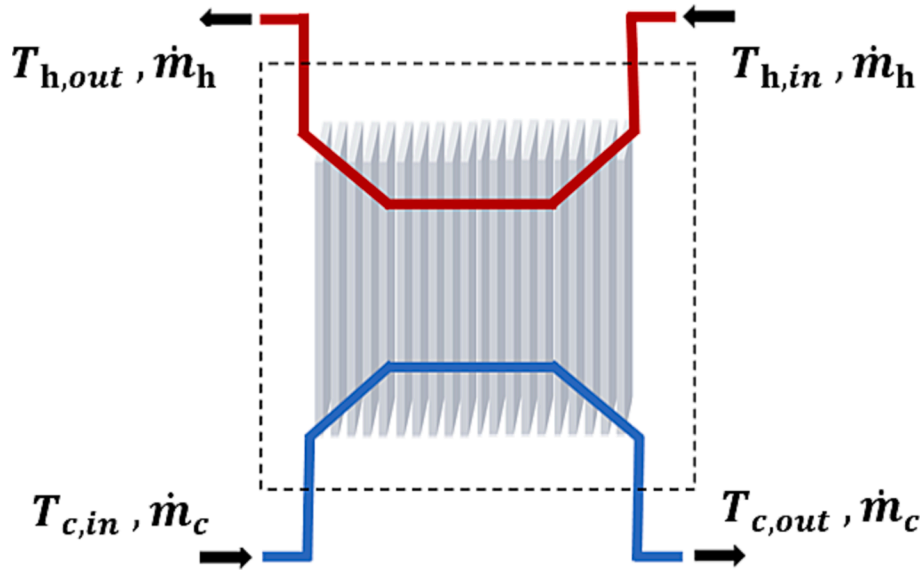


**Fig. 4.** Unit operation for a heat exchanger, indicating the inlet and outlet stream temperatures and flowrates, Where,  $\dot{m}$ ,  $T_{in}$  and  $T_{out}$  are the mass flowrate, the inlet and the outlet temperature of the stream in one the cold (c) or hot (h) side of the heat exchanger.

exchanger,  $\dot{Q}_{exchange}$ . This is equal to the difference in enthalpy rate between the inlet and outlet stream from one side of a heat exchanger,  $\Delta\dot{H}$  [48].

$$\dot{Q}_{exchange} = \Delta\dot{H} \quad (9)$$

The next step estimated the overall heat transfer coefficient,  $U_{he}$  [45]. Given  $U_{he}$ , the total heat exchange surface,  $A_{he}$  can be estimated from Eq. (10), and the total number of plates,  $N_{pt}$  can be determined from Eq. (11) given the surface area of a plate,  $A_{pt}$ . Values for the plate dimensions and other geometrical characteristics of plates used for the calculations were extracted from the study of Mehrabian et al. (2000) [49].

$$A_{he} = \frac{\dot{Q}_{exchange}}{U_{he}} \quad (10)$$

$$N_{pt} = \frac{A_{he}}{A_{pt}} \quad (11)$$

### 2.1.3. Pipeline diameter selection

The pipeline diameter for a processing line is scaled based on the processing flowrate. All unknown flowrates of the processing unit of Fig. 2 were evaluated following the steps presented in Section 2.1.1 and 2.1.2. To find an approximation for the required ideal pipeline diameter at a given the flowrate, the Adam's equation [50] was used (Eq. (12):

$$d_{id} = 0.25 \sqrt{\dot{V}} \quad (12)$$

Where,  $\dot{V}$  is the stream volume flowrate measured in gal/min and  $d_{id}$  is the ideal pipeline diameter measured in inches. However, the pipeline diameter selected should be one commercially available with the closest diameter to  $d_{id}$ . Thus, the appropriate standardised pipeline diameter  $d_{st}$  was used for any further calculations [51].

### 2.1.4. Energy demand for the cleaning-in-place process

Faced by the dairy industry in liquid dairy heat treatment processes is when proteins, fats, and minerals coagulate on the surface of the heat exchanger walls – a phenomenon called fouling [52]. Dairy fouling is a

result of reaction of dairy components, mainly casein proteins occurring in the bulk flow and on top of the heat exchange surfaces during thermal treatment at temperatures higher than 70 °C [53]. Fouling acts as a thermal insulator affecting heat exchange during processing and can also act as a substrate for the growth of microorganisms over time, which will cause an impact on quality (and potentially safety) [54,55]. In order to remove fouling, the pasteurisation process needs to be interrupted at regular intervals, every 8–10 h, to allow for the cleaning of the inner processing line surfaces by pumping cleaning fluids, an automated process called cleaning-in-place (CIP) [42,56].

For the needs of this study, the CIP programmes including CIP for pasteurisers, disinfection, and cold components as described in the Tetrapack Handbook for pasteurisation lines [42] was used to calculate the CIP energy consumption. The CIP programme for a pasteuriser has the following steps:

1. 10 Minutes rinsing with warm water.
2. 30 min circulation with an alkaline detergent solution (0.5 – 1.5 % (w/w)) at 75 °C. Usually, 1% (w/w) sodium hydroxide (NaOH) is used to dissolve deposit proteins and acts as bactericide [57].
3. 5 Minutes rinsing out the alkaline detergent with warm water.
4. 20 min circulation of an acid solution (0.5 – 1.0 % (w/w)) at 70 °C. Usually, nitric (HNO<sub>3</sub>) or phosphoric acid (H<sub>3</sub>PO<sub>4</sub>) is used in order to remove deposited salts [57].
5. Post-rinsing with cold water (to remove all trace of detergent, note duration is not detailed in source [42]).
6. 8 Minutes cooling with cold water.

The CIP programme for disinfection takes place once a day in the morning and is performed by circulating hot water at a temperature between 90–95 °C for a duration of 10 to 15 min until the returning temperature reaches at least 85 °C.

Finally, a cleaning-in-place (CIP) programme for “cold components” of the processing line, such as pipes and tanks, is performed once a day following the steps below:

1. Flushing with warm water for three minutes
2. 10 Minutes circulation of an alkaline detergent solution (0.5 – 1.5 % (w/w)) at 75 °C
3. Rinsing with warm water for three minutes
4. 5 min disinfection using hot water at 90 to 95 °C
5. 10 min gradual cooling by utilising cold tap water (typically excluding cooling for tanks)

The CIP system pumps cleaning fluids along the processing line at a sufficient velocity to achieve turbulent flow, as the turbulence increases the fluid shear at the internal surface, which achieves more effective cleaning. The flow velocity of the cleaning fluids pumped into the pipeline,  $u_{cf}$  should range between 1.5 and 3.0 m/s [58]. Eq. (13) was used to calculate the required mass flow rate,  $\dot{m}_{cf}$  of the cleaning fluid, given the cleaning fluid velocity,  $u_{cf}$  and the standardised pipeline diameter,  $d_{st}$  of the processing line as calculated in Section 2.1.3.

$$\dot{m}_{cf} = \pi \frac{d_{st}^2}{4} u_{cf} \rho_{cf} \quad (13)$$

Where,  $\dot{m}_{cf}$  is the mass flowrate of the cleaning fluid and  $\rho_{cf}$  is the density of the cleaning fluid assuming to be equal to that of water.

The energy required to heat up the cleaning fluids was calculated using Eq. (14):

$$\dot{Q}_{cf,n} = \dot{m}_{cf} \int_{T_{cf}}^{T_{cf,amb}} C_{p,cf} dT \quad (14)$$

Where,  $\dot{Q}_{cf,n}$  is the heating energy required to heat the cleaning fluid of each step  $n$  of the CIP programme.  $T_{cf,amb}$  are the initial cleaning fluid temperature at room temperature and  $T_{cf}$  is the temperature of the

cleaning fluid. For reasons of simplicity, the specific heat capacity of the cleaning fluid  $C_{p,cf}$  and density  $\rho_{cf}$  were considered to be equal to that of water.

After calculating the required heat to be provided in each cleaning fluid, the total heating energy  $Q_{cleaning}$  required for cleaning was calculated through Eq. (15):

$$Q_{cleaning} = \sum_n \dot{Q}_{cf,n} t_{cf,n} \quad (15)$$

Where,  $t_{cf,n}$  is the time of cleaning of the cleaning step  $n$  measured in seconds.

#### 2.1.5. Pressure state calculation

Pumps are equipment used to transfer fluids between processing equipment. They are also responsible for regulating the pressure level, which is continuously dropping due to friction within the process line inner walls during the recirculation of fluids through piping and process equipment. Heat exchangers affect the energy consumption of the dairy processing plant indirectly, because the flow of the inlet streams through narrow flow channels of complex geometry leads to turbulent flow, which results in substantial pressure drop. The pressure drop is recovered by pumps placed along the process line.

The pressure drop due to flow through the heat exchangers was modelled as described in Section 2.1.5.1, and the pressure drop as a result of stream passing through the processing lines was modelled as described in Section 2.1.5.2. After defining the pressure drop resulting from each heat exchanger and processing line section, the pressure in the outlet of each pump was chosen to provide sufficient pressure rise. This is to ensure the pressure does not drop below the vapour pressure of the liquid along the pipeline, which would result in bubble formation or cavitation that could damage the process equipment causing erosion and is also associated with increasing fouling effects [53,58].

**2.1.5.1. Pressure drop from plate heat exchangers.** For the pressure drop calculation through the PHEs, the Gusew & Stuke (2019) model was used [59]. This model accounts for the pressure drop across the corrugated plates' channels, the pressure drop caused by distribution ducts, and the pressure drop due to elevation change under turbulent flow at different corrugation angles for plates. The corrugation angle was chosen to be 63° since this angle resulted in the highest pressure drop compared to smaller corrugation angles [59]. For the pressure drop calculation in each fluid side of the heat exchanger, material properties were calculated according to the property models of section A in the Supplementary Material for the average temperature between the inlet and outlet.

**2.1.5.2. Pressure drop from pipeline.** The pressure drop through the pipeline was calculated through the evaluation of the friction factor  $f_p$  of the pipeline, given the diameter of the pipeline  $d_{st}$  (as calculated in Section 2.1.3), and the Reynolds number  $R_e$  (Eq. (16), Eq. (17) & Eq. (18)) [50].

$$\frac{1}{\sqrt{f_p}} = -2 \log \left( \frac{\epsilon}{3.7 d_{st}} + \frac{2.51}{R_e \sqrt{f_p}} \right) \quad (16)$$

Where  $R_e$  is given from:

$$R_e = \frac{\rho u d_{st}}{\mu} \quad (17)$$

Where,  $\rho$  is the fluid density,  $u$  is the fluid velocity,  $\mu$  is the fluid dynamic viscosity and can be calculated for the different fluids as shown in Section A in the Supplementary Material.

Given the estimated friction factor  $f_p$ , the pressure drop due to flow in the pipeline  $\Delta P_p$  can be calculated given the length of the pipeline  $L$ , through Eq. (18) [50].

$$\Delta P_p = f_p \rho \frac{u^2}{2} \frac{L}{d_{st}} \quad (18)$$

## 2.2. Modelling cold storage facilities

The energy consumption of the refrigerated facilities across dairy manufacturing and distribution depends on several factors such as the ambient and storing temperature conditions, the storage wall materials and the initial temperature of the stored products. To account for the impact of those factors on energy use, a mechanistic modelling approach was followed.

### 2.2.1. Thermal load on refrigerated facilities

In any cold storing facility, electrical energy is consumed by the refrigeration system, which is responsible for discharging the total thermal load,  $Q_T$  posed on the system, in order to regulate the storage temperature. **Section 2.2.1.1** presents the method followed to evaluate the thermal load ( $Q_T$ ) on the cooling tanks used for raw milk prior to manufacturing commencing, and **Section 2.2.1.2** for the cold storage chamber in manufacturing and for the refrigerated unit of the refrigerated vehicles.

**2.2.1.1. Thermal load on cooling tank.** The thermal load,  $Q_{T,ct}$  on the cooling tank for raw milk cold storage (T-101 in Fig. 2) is a result of the heat released during cooling of the raw milk,  $Q_{rmc}$  and due to the heat transmission through the tank walls,  $Q_{tw}$  (Eq. (19)).

$$Q_{T,ct} = Q_{rmc} + Q_{tw} \quad (19)$$

$Q_{rmc}$  is calculated through Eq. (20):

$$Q_{rmc} = m_{rm} C_{p,rm} (T_{cs} - T_{rm,i}) \quad (20)$$

Where,  $m_{pr}$  is the total mass of raw milk in the cooling tank,  $C_{p,rm}$  is the specific heat capacity of raw milk stored,  $T_{rm,i}$  the initial temperature of raw milk loaded in the cooling tank, and  $T_{cs}$  the cold-storage temperature [60,61].

$Q_{tw}$  is calculated through Eq. (21):

$$Q_{tw} = U_{tw} A_{tw} (T_{amb} - T_{cs}) \quad (21)$$

Where,  $U_{tw}$  is the overall heat transfer coefficient for the tank wall, and  $A_{tw}$  is the heat exchange surface of the tank calculated as presented in the study [60], and  $T_{amb}$  is temperature outside of the tank.

**2.2.1.2. Thermal load on cold storage chamber and the refrigeration unit of refrigerated vehicle.** The thermal load,  $Q_{T,CS}$  on the cold storing chambers and the refrigeration unit of the vehicles, is a result of the heat released during product cooling ( $Q_{pr}$ ), the heat transmission through the enclosures ( $Q_{en}$ ), door openings ( $Q_{do}$ ), from the heat released from people entering the storage chamber  $Q_{pe}$ , and from the heat released by electrical equipment such as light bulbs and circulation air fans ( $Q_{ele}$ ) (Eq. (22)).

$$Q_{T,CS} = Q_{pr} + Q_{en} + Q_{do} + Q_{pe} + Q_{ele} \quad (22)$$

The  $Q_{en}$  is a temperature dependent variable and is calculated similarly to the approach for the cooling tank as follows:

$$Q_{en} = U_{en} A_{en} (T_{amb} - T_{pr}) \quad (23)$$

Where,  $U_{en}$  is the overall heat transfer coefficient of the chamber or refrigeration unit enclosures, which was calculated as presented in [62] and [63] respectively, and  $A_{en}$  is the heat exchange surface of the enclosure,  $T_{pr}$  is the storing temperature of products in the cold storing chamber and  $T_{amb}$  is the ambient temperature or the temperature outside of the storage chamber. More details on calculating the thermal load for cold storage chambers and refrigeration units of vehicles can be found in [62] and [63] respectively.

## 2.3. Energy usage of electrical or fuel-powered equipment

This section presents the formulae used to calculate the power demand of electrical and fuel-powered equipment for milk and cream manufacturing and distribution. This equipment involves pumps (Section 2.3.1), steam, compressed air, chilled water, and cold water supply systems (Section 2.3.2), the centrifugal separator (Section 2.3.3), the homogeniser (Section 2.3.4), the packaging process (Section 2.3.5), the refrigeration systems (Section 2.3.6), and the refrigerated vehicles (Section 2.3.7).

### 2.3.1. Energy model for pumps

The electric power consumption of a pump  $\dot{W}_{pump}$  are given from [55]:

$$\dot{W}_{pump} = \frac{\dot{m}_{pump} g H_{pump}}{\eta_{pump} \eta_{p,el,mot}} \quad (24)$$

Where,  $\dot{m}_{pump}$  the mass flow rate of the pumped stream,  $g$  is the gravity acceleration,  $\eta_{pump}$  is the pump energy efficiency, and  $\eta_{p,el,mot}$  is the efficiency of the electric motor of the pump (Eq. (27)).  $H_{pump}$  is the total head of a pump, which represents the height that a pump can raise water upwards and is given by the desired pressure rise  $|\Delta P_{pump}|$  evaluated as described in Section 2.1.5, and the density of the pumped fluid  $\rho_{pump}$  using the following equation:

$$H_{pump} = \frac{|\Delta P_{pump}|}{\rho_{pump} g} \quad (25)$$

In industrial process design, pump selection is performed by using operating graphs, provided by the pump manufacturers that indicate the most appropriate pump for each application and provide the pump efficiency. In the dairy industry, centrifugal pumps are most commonly used for liquids [42]. Instead of using pump performance graphs, Eq. (26) offers a broad estimation for centrifugal pump efficiency,  $\eta_{pump}$  given the total head of pump,  $H_{pump}$  and the volume flow rate of stream entering the pump,  $\dot{V}_{pump}$  [64].

$$\eta_{pump} = (80 - 0.937 H_{pump} + 5.460 \bullet 10^{-6} \dot{V}_{pump} H_{pump} - 1.514 \bullet 10^{-11} \dot{V}_{pump}^2 H_{pump}^2 + 5.802 \bullet 10^{-3} H_{pump}^2 - 3.028 \bullet 10^{-14} \dot{V}_{pump}^2 H_{pump}^2) \quad (26)$$

Finally, the electric motor efficiency,  $\eta_{p,motor}$  is calculated using Eq. (27), which is derived from data for the electric motor efficiency,  $\eta_{p,el,mot}$  for different pump power values,  $\dot{W}_{pump}$  provided in [65]:

$$\eta_{p,el,mot} = 0.815 + 0.00206 \ln(\dot{W}_{pump}) \quad (27)$$

### 2.3.2. Steam, compressed air, chilled water and cold water supplies

In the milk and cream processing units, steam is used to heat up the hot water recirculating systems through the heat exchangers, E-107 and E-206 (Fig. 2). Steam is also used in the packaging process to disinfect the product packaging before it is filled. Steam is produced by a boiler system which burns fuel. In the packaging process, compressed air is used for plastic bottle moulding and filling. Compressed air supply is produced via an oil-injected air compressor that uses electricity [58]. Regarding the cooling needs in the milk and cream processing units, chilled water is supplied in the E-102 and E-202 heat exchangers in order to cool down pasteurised skimmed milk and cream to prevent microbial growth. Chilled water is produced in a chilled water system, which includes a chiller, a cooling tower, a chilled water pump and an electrically powered condenser water pump [66]. Moreover, in the cream processing unit, cold water is supplied via a cooling tower, (CT-201 in Fig. 2). For the evaluation of the energy requirements for these supplies, benchmarking values were used. More specifically, COP values for the steam, compressed air, chilled water and cold-water supply

systems in food manufacturing were used which are presented in **section B** in the [Supplementary Material](#) [66,67].

### 2.3.3. Energy model for centrifugal separator

To estimate the power consumption of a centrifugal separator, a simplified version of the Szepessy and Thorwid model was used to estimate the power usage of the separator device and the power of the inlet feed pump [60]. According to this study, the overall power consumption,  $\dot{W}_{tot.sep}$  is equal to the sum of the power used by the pump,  $\dot{W}_{pump.sep}$  and the power consumption of the separator device,  $\dot{W}_{cent}$ :

$$\dot{W}_{tot.sep} = \dot{W}_{pump.sep} + \dot{W}_{cent} \quad (28)$$

In the above study [60], a combination of analytical and data-driven approaches for energy evaluation are provided. Whilst in the present study, the Szepessy and Thorwid energy model was simplified by applying polynomial regression to the data provided in their study for the calculation of the absolute pressure drop,  $|\Delta P_{sep}|$  and the centrifugal separator power,  $\dot{W}_{cent}$  as a function of the inlet volume flowrate. The regression models are presented in **section C** in the [Supplementary Material](#). Given  $|\Delta P_{sep}|$  and  $\dot{W}_{cent}$ , **Eq. (29)** was applied to provide the power needs of the inlet feed pump  $\dot{W}_{pump}$  for **Eq. (28)** [60].

$$\dot{W}_{pump} = \frac{\dot{m}_{sep} |\Delta P_{sep}|}{\eta_{pump.sep}} \quad (29)$$

Where,  $\dot{m}_{sep}$  is the mass flow rate of the inlet stream of the separator  $|\Delta P_{sep}|$  is the pressure rise of the pump in the centrifugal separator and  $\eta_{pump.sep}$  is the pump efficiency taken equal to 0.88 [68].

### 2.3.4. Homogeniser energy

Homogenisation aims to produce more stable fat emulsions in order to prohibit gravitational separation of fat in the milk or cream outlet stream [48]. Homogenisation is achieved with a high-pressure pump, which pumps the milk or cream through narrow gaps causing turbulence and cavitation effects that lead to the desired breakdown of fat globules. To estimate the power demand of the homogeniser,  $\dot{W}_{hom}$  the following equation, **Eq. (30)** was used [42]:

$$\dot{W}_{hom} = \frac{\dot{m}_{hom} |\Delta P_{hom}|}{\eta_{hom} \eta_{el.mot}} \quad (30)$$

Where,  $\dot{m}_{hom}$  is the mass flow rate of the inlet stream to the homogeniser,  $|\Delta P_{hom}|$  is the pressure rise resulted by the stream passing through the homogeniser,  $\eta_{hom}$  is the pump efficiency of the homogenizer equal to 0.85 and  $\eta_{el.mot}$  is the electric motor efficiency equal to 0.95 [42].

### 2.3.5. Packaging energy use

Currently, plastic packaging is the most widely used packaging for milk and cream products worldwide, and thus was the type of packaging considered in the model. Although there has been a recent increase in carton packaging, especially in European markets, this study selects to demonstrate the energy quantification for the use of plastic packaging. However, subject to data availability, alternative and/or more sustainable packaging could also be considered in this model to assess their energy consumption. To evaluate the energy use of the plastic packaging process, data from an LCA study of different packaging systems was used. Specifically, the study provided benchmarking values for the electricity, steam, and compressed air demand for the packaging processes involving the demand for the packaging decontamination, filling and capping processes [69]. The data were estimated by collecting information from three manufacturers of filling machines, and four dairy plants using these machines. It is important to note that the energy use of packaging in this study refers to the energy consumption within dairy manufacturing and does not involve the energy used for the packaging's primary materials or the production of bottle preforms. **Table 1** contains the values of the electricity, steam and compressed air consumption per unit of plastic package using HDPE and PET bottles [69].

**Table 1**

Electricity, steam and compressed air demand for ultra-clean filler plastic packaging systems per unit of HDPE and PET bottles [69].

Electricity ( $10^{-3}$ kWh)	2.59
Steam ( $10^{-3}$ kg)	2.46
Compressed air ( $10^{-3}$ N/m <sup>3</sup> )	9.78

### 2.3.6. Electricity demand for refrigeration

The refrigeration systems principally works through an evaporation-compression cycle of a refrigerant fluid [62]. The electrical energy  $E_{cf}$  required to power the refrigeration system of a cooling facility can be estimate from **Eq. (31)**:

$$E_{cf} = \eta_{mc} COP_{comp} Q_T \quad (31)$$

Where,  $\eta_{mc}$  is the efficiency of the motor of the compressor taken equal to 91% as an average value in the results of [70], and  $COP_{comp}$  is the COP of the compressor of the refrigerant system can be calculated from **Eq. (32)** [62]:

$$COP_{comp} = \frac{0.5(T_{evap} + 273.15)}{T_{cond} - T_{evap}} \quad (32)$$

Here,  $T_{evap}$  is the average temperature of the evaporator ( $^{\circ}$ C) assumed to be equal to the cold storing temperature  $T_{cs}$  and  $T_{cond}$  is the average temperature of the condenser taken equal to  $55^{\circ}$ C [62].

### 2.3.7. Transportation energy model

After products are produced, refrigeration transportation is required to transfer the products from dairy plants to distribution centres and from distribution centres to the retail outlets. In this study, two categories of refrigerated vehicles were modelled: diesel and electric-powered. The refrigerated vehicles require energy for transportation  $E_{tr}$  which was calculated as presented in **Section 2.3.7.1** and for refrigeration  $E_{re}$  which was calculated as presented in **Section 2.3.7.2**.

$$E_{rv} = E_{tr} + E_{re} \quad (33)$$

Where,  $E_{rv}$  is the total diesel- or electric-energy consumed by a refrigerated vehicle.

**2.3.7.1. Energy consumption for transportation.** For the evaluation of the transportation energy consumption  $E_{tr}$ , benchmarking values were used. Specifically, for the diesel-powered vehicles, Tassou et al., (2009) [71] provided benchmarking values for the average fuel consumption per tonne of transported product and kilometres travelled for different types of vehicles. For the electric-powered vehicles the respective benchmarking values for electric-powered vehicles were used [72]. The benchmarking values for different types of diesel- or electric-powered refrigerated vehicles are provided in **Table 2** [71].

To estimate the diesel or electricity demand for transportation  $E_{tr}$ , the linear relationship of **Eq. (34)** was applied.

$$E_{tr} = d \bullet E_i \bullet m_p \quad (34)$$

Here,  $d$  is the transportation distance of a route,  $E_i$  is the benchmarking value for the energy intensity per unit of distance and mass of load (provided in **Table 2**), and  $m_p$  is the mass load of product transported which was given equal to the average payload of **Table 2**.

**2.3.7.2. Energy consumption for refrigeration in vehicle.** The energy consumption for refrigeration resulted for the evaluation of the thermal load for the refrigeration unit  $Q_T$  as presented in **Section 2.2.1**. Then, the electricity demand for refrigeration  $E_{cf}$  can be evaluated from the thermal load, as presented in **Section 2.3**. For the case of diesel-powered refrigerated vehicles, the electrical energy for refrigeration  $E_{red}$  is provided by the electric generator of the vehicle which typically has an efficiency  $\eta_{ge}$  around 0.4 (**Eq. (35)**) [73]:

**Table 2**

Average payload and energy intensity and of refrigerated vehicles based on their class [71,72]. Where average payload stands for the average load carried by a vehicle exclusive of what is necessary for its operation which corresponds to the total product transported weight.

Vehicle Category	Vehicle class	Average payload [tonnes] (Weight of the products when vehicle fully loaded)	Energy intensity by weight and distance	Units	Reference
Diesel	Medium rigid	2.25	83.8	$\frac{ml}{tonnekm}$	[71]
	Large rigid	7.41	37.1	$\frac{ml}{tonnekm}$	[71]
	City-articulated	6.57	36.4	$\frac{ml}{tonnekm}$	[71]
	32-tonne articulated	10.37	26.4	$\frac{ml}{tonnekm}$	[71]
	38-tonne articulated	11.83	26	$\frac{ml}{tonnekm}$	[71]
	Full electric truck class 8 UDDS	11.8	0.1135	$\frac{kWh}{tonnekm}$	[72]
Electric	Full electric truck class 8 Regional 500	11.8	0.1254	$\frac{kWh}{tonnekm}$	[72]

$$E_{red} = E_{cf} \eta_{ge} \quad (35)$$

In the case of an electric-powered refrigerated vehicle, the electric energy for refrigeration derives directly from the vehicle's battery with an approximately 94–98% DC-DC convertor efficiency, (where DC stands for direct currency), while the onboard charger efficiency  $\eta_{charging}$ , which is the efficiency to store electricity from the grid into the vehicles battery, has a value of 97–98% [74]. Thus, as a brief approximation the electric energy required from the grip allocated for refrigeration is given from Eq. (36):

$$E_{reel} = \eta_{DC-DC} \eta_{charging} E_{cf} \quad (36)$$

## 2.4. Total manufacturing and distribution energy consumption evaluation

This section provides the methodology for how the energy consumption models for the different operations along skimmed milk and cream manufacturing and distribution were integrated, in order to evaluate the total energy consumption and related carbon emissions.

### 2.4.1. Product-embodied energy

The product-embodied energy  $E_{unit}$  was estimated by calculating the total energy requirements of each individual operation involved in manufacturing and distribution that correspond to a unit of product. Since skimmed milk and cream products have some common processes (such as milk separation, storage and transportation), the energy needed to be allocated based on the mass rate of each product. Thus,  $E_{unit}$  was calculated using Eq. (37).

$$E_{unit} = m_{unit} \sum_k \frac{CV_k \dot{W}_k}{\dot{a}_k} + m_{unit} \sum_k \frac{CV_k E_k}{m_k} \quad (37)$$

Where,  $m_{unit}$  is the mass of a product unit, and for each process or equipment  $k$  used in product manufacturing and distribution,  $\dot{W}_k$  is the electrical or fuel power consumption of a continues process  $k$ ,  $CV_k$  is the gross calorific value of the used fuel for the process  $k$  provided in Table 3 [75,76] and  $\dot{a}_k$  is the rate of mass that is treated through the process or equipment  $k$  per second. While  $E_k$  is the energy consumption of an operation, and  $m_k$  is the total product mass treated through this

**Table 3**

Gross calorific value of the used fuel [75,76].

Type of fuel	Gross calorific value of the used fuel or electricity	Reference	Unit
Oil burning fuel	46.17	[75]	GJ/tonne
Natural Gas	40.23	[75]	GJ/tonne
Hydrogen	141.7	[76]	GJ/tonne
Diesel for transportation	45.29	[75]	GJ/tonne

operation.

### 2.4.2. Product carbon footprint from energy use

The carbon footprint from energy use  $CF_{unit}$  for each product can be estimated with a similar method to that of the product-embodied energy of Section 2.4.1. Here, in order to express the energy use in carbon dioxide equivalent emissions ( $CO_2e$ ), carbon conversion factors  $f_c$  from the UK Government for each energy resource between electricity, oil, diesel, natural gas were used (Table 4) [77]. The type of hydrogen assumed to be used in this study is “green hydrogen”, which is produced explicitly from renewable energy resources. Although ranges for the carbon conversion factor of green hydrogen produced using different green technologies were available in the literature, in this study it is assumed that the carbon conversion factor of green hydrogen is equal to 2.2 kg $CO_2e$ /kg $H_2$  [78]. This assumption was made based on the general rule-of-thumb that the carbon footprint of green hydrogen should be at least 5 times lower than the respective value of grey hydrogen, which is a well-established footprint in literature and has the value of 11.5 kg $CO_2e$ /kg $H_2$  [78]. This value correlates well with the UK's value for carbon conversion factor of green hydrogen which was equal to 2 kg $CO_2e$ /kg $H_2$  [23]. As the technology for hydrogen production matures and becomes available on a commercial scale, more data of the carbon conversion factor of hydrogen will become available. However, a detailed methodology for the estimation of the carbon conversion factor of hydrogen is provided in a recent UK Government paper [79]. The carbon conversion factor of electricity is not a steady value but is expected to drop over the years by 80% by 2050 due to the electricity decarbonisation plan (Table 5) [77]. Due to this alteration, the product's carbon footprint from energy,  $CF_{unit}$  should be evaluated for a specific year of reference, as shown in Eq. (38):

$$CF_{unit}(year) = m_{unit} \sum_k \frac{f_c(year) CV_k \dot{W}_k}{\dot{a}_k} + m_{unit} \sum_k \frac{f_c(year) CV_k E_k}{m_k} \quad (38)$$

### 2.4.3. Annual manufacturing and distribution carbon emissions from energy use

The assessment of the environmental impact of the energy used for manufacturing and distribution in this study was performed by evaluating the system's annual energy derived carbon emissions,  $CF_{system}$  from Eq. (38). The  $CF_{system}$  is evaluated for a specific year reference due to the electricity decarbonisation plan [77] (see prior Section 2.4.2).

$$CF_{system}(year) = n_{tot,SM} CF_{unit,SM}(year) + n_{tot,C} CF_C(year) \quad (39)$$

Where,  $n_{tot,SM}$  and  $n_{tot,C}$  is the total number of skimmed milk and cream products respectively produced annually, and  $CF_{unit,SM}$  and

**Table 4**

Carbon conversion factor for different fuels [77,78].

Type of fuel	Carbon conversion factor [kg $CO_2e$ /tonne]	Reference
Oil burning fuel	3165.04	[77]
Natural Gas	2539.51	[77]
Hydrogen	2200	[78]
Diesel for transportation	3228.89	[77]

**Table 5**

Projections for grid average industrial electricity emission factors towards 2050 [77].

Year	Carbon conversion factor [kg CO <sub>2</sub> e/kWh] [77]
2020	0.135
2025	0.101
2030	0.080
2035	0.039
2040	0.039
2045	0.033
2050	0.027

$CF_{unit,C}$  is the carbon footprint from energy use of a unit of skimmed milk and cream product respectively.

Future projections of the energy derived carbon emissions from dairy manufacturing and distribution can be done by evaluating the  $CF_{system}$  towards 2050. This can facilitate the creation of a roadmap towards the net zero carbon target.

## 2.5. Scenario analysis

The simulation flexibility offered by the mechanistic approach in the presented model allowed for the investigation of the products' energy use and related carbon emissions under different scenarios. Specifically, 12 different manufacturing and distribution scenarios were simulated. These scenarios resulted from the combination of three types of fuel used for the heating needs at the manufacturing plant, two categories of refrigerated vehicles, and two types of distribution system infrastructures (Fig. 5).

The carbon impact of product manufacturing depends mainly on the energy sources used in manufacturing [80]. Thus, three types of combustion fuels for the heating requirements in dairy manufacturing were considered in the scenario analysis, being oil, natural gas, and hydrogen [81]. Traditionally, oil burning boilers were used to produce hot water or steam and past years has seen their gradual replacement with natural

gas burning boilers. However, oil combustion is still used in old and/or smaller-scale dairy plants or in locations where there is no access to the natural gas network. The motivations to move to natural gas is because its combustion produces reduced and cleaner emissions compared to those of oil fuel [82]. Hydrogen fuel use was also simulated, since it is a low- or zero-carbon fuel, which has a strong potential to be used as combustion fuel in industrial sectors in the future, offering a key solution towards achieving net zero targets [20,83].

Regarding the distribution stage, the products' energy use and carbon impact depends on the type of refrigeration vehicle used, and the distribution distance covered. Thus, to understand how the electrification of transportation can limit the system's carbon emissions, two categories of refrigerated vehicles were simulated in the scenario analysis, diesel- and electric- powered.

In addition, to study different dairy distribution configurations, centralised and decentralised were considered in the scenario analysis. Centralised production systems were represented by a large sized dairy that processes 50,000 L of raw milk per hour and with product distribution through nationwide routes of a total average distance of 550 km (500 km with long-haul refrigerated vehicles from the manufacturing plant to the distribution centre and 50 km from the distribution centre to the retail outlet using city refrigerated vehicles) (Fig. 6). Decentralised production systems were represented by simulating 5 small sized dairy manufacturing plants that process 10,000 L of raw milk per hour and distributes their products through regional routes of total average distance from the dairy plant to the retail outlet of 100 km (50 km with long-haul refrigerated vehicles from the dairy to the distribution centre and 50 km with city refrigerated vehicles from the distribution centre to the retail outlet) (Fig. 7). The production capacity of the large dairy plant used to represent the centralised production system (50,000 L/h) being equal to the summation of the processing capacities of all five smaller dairy plants used to represent a decentralised distribution system (10,000 L/h processing capacity each), so that the modelled systems are comparable with each other in the following Scenario Analysis in Section 3.

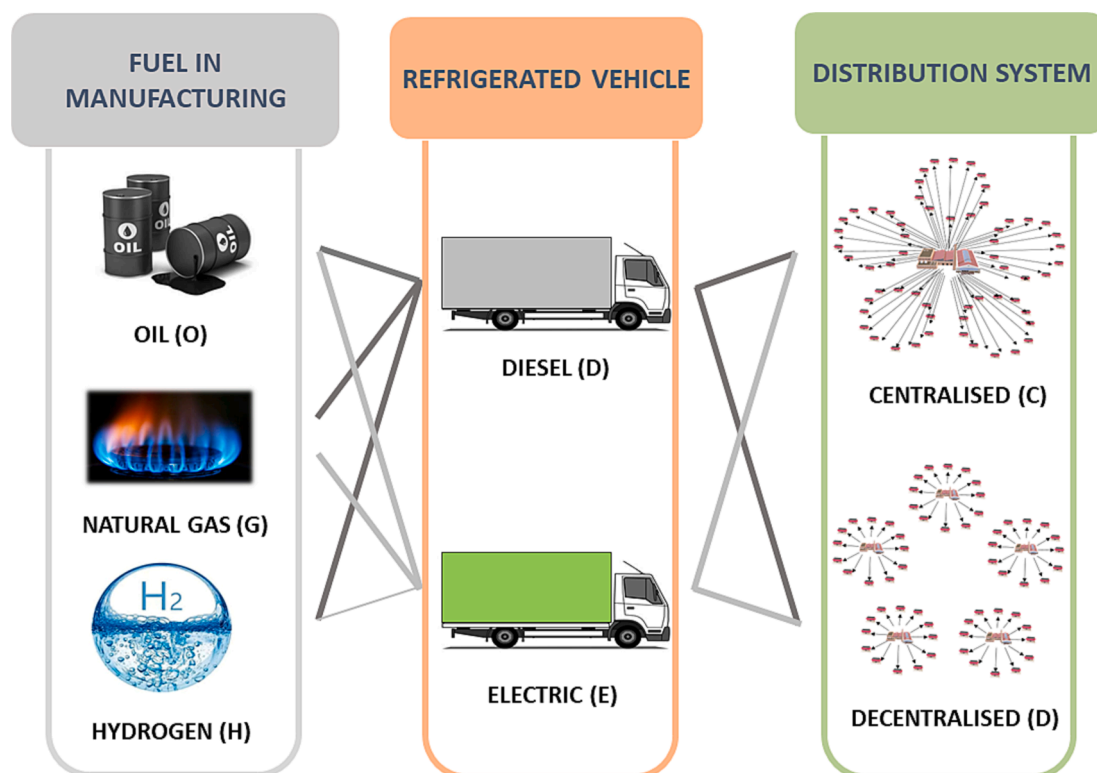


Fig. 5. Manufacturing and distribution scenarios' acronyms scheme.

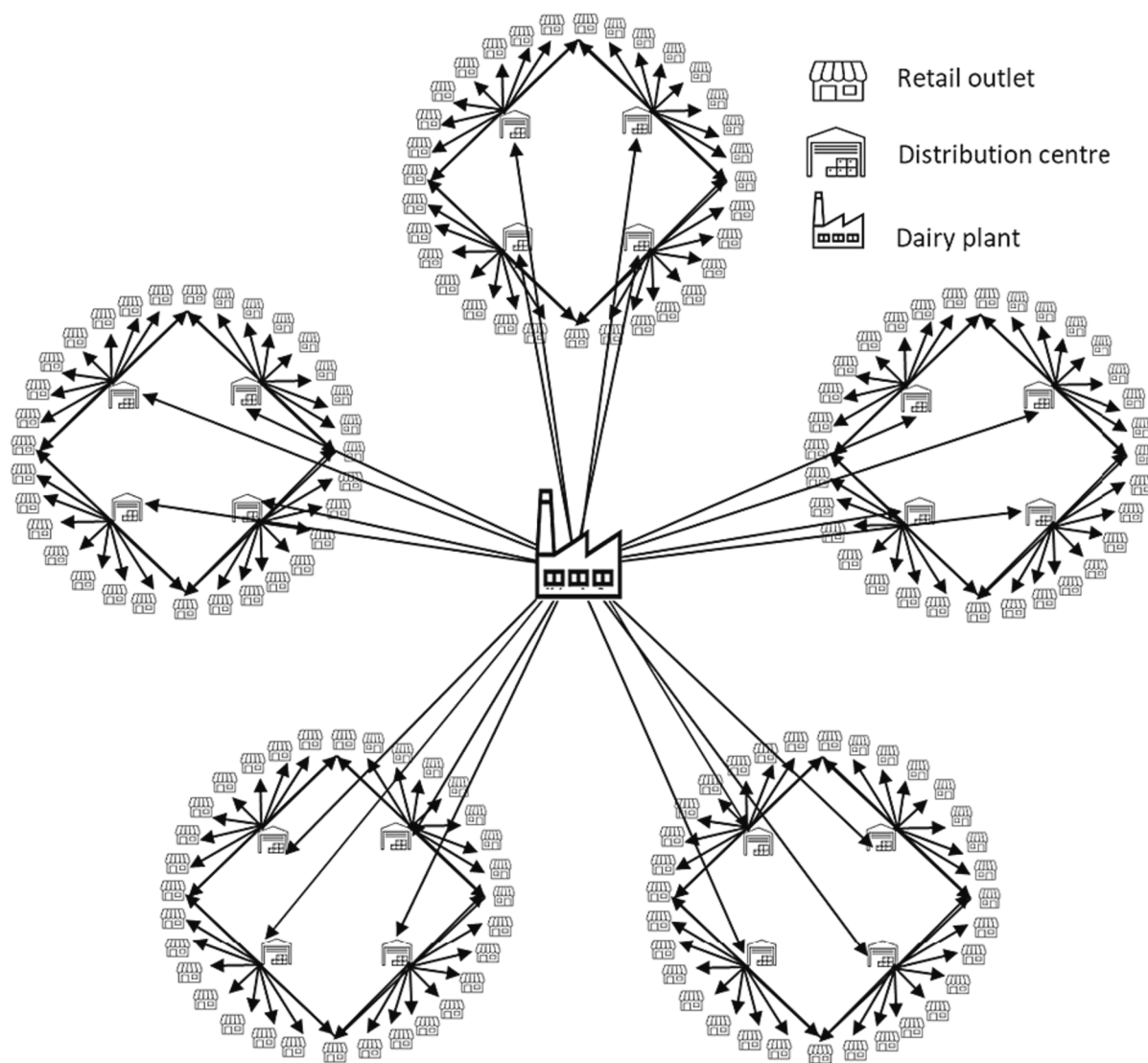


Fig. 6. Schematic of a centralised milk and cream production system.

The dairy plants simulated were operational for 16 h per day (8 h of processing followed by a CIP programme for the pasteurisers of the milk and cream production line twice a day) for 260 days per year, representing a typical dairy manufacturing facility [35]. Moreover, the size of the dairy plant was categorised as small or large according to the study of Tomasula et al., (2013) [35]. Moreover, in this study it is assumed that the ambient temperature is 20 °C and the cold storage temperature of both raw milk and cream products is 4 °C [42].

The 12 scenarios simulated were named using 3-letter acronyms as described in Fig. 5 and Table 6. In the following scenario analysis, the scenarios are ordered from those anticipated to be the highest carbon emitting to the lowest.

### 3. Results and discussion

This section presents and discusses the scenario analysis undertaken for the manufacturing and distribution of 1 L skimmed milk and 330 ml cream products. Section 3.1 presents the results for the product-embodied energy evaluated according to the method presented in Section 2.4.1. Section 3.2 presents the energy mapping and carbon footprinting by energy source results, evaluated following the methodology of Section 2.4.1 and 2.4.2. Finally, Section 3.3 presents the projections of dairy manufacturing and distribution carbon emissions by 2050,

evaluated following the methodology of Section 2.4.3.

#### 3.1. Quantifying product-embodied energy and energy mapping

To examine the product-embodied energy (see Section 2.4.1) for skimmed milk and cream, simulations were undertaken for 12 different manufacturing and distribution scenarios (Table 6). The results for the product-embodied energy for 1L of skimmed milk (0.08% w/w fat content) and 330 ml of cream (38% w/w fat content) are presented in Figs. 8 and 9 respectively. According to the simulation results, the product-embodied energy of skimmed milk ranged from 365 to 917 kJ per L (Fig. 8), while the embodied energy of cream ranged from 211 to 403 kJ per 330 ml (Fig. 9).

When considering only the manufacturing stage, the energy consumption ranges between 261 and 316 kJ per L for skimmed milk products and between 135 and 179 kJ per 330 ml for cream products. Comparatively, an LCA study on milk manufacturing in Denmark evaluated milk product-embodied energy from 430 to 1500 kJ/kg [84], whilst reported values for milk dairies in US, Canada, Australia and Europe for the milk product-embodied energy ranged from 200 to 6,000 kJ/kg for fluid milk manufacturing [25,32]. It is worth mentioning that the model does not show significant differences (<1%) in energy use for manufacturing at different scales of production (50,000 L/h in versus

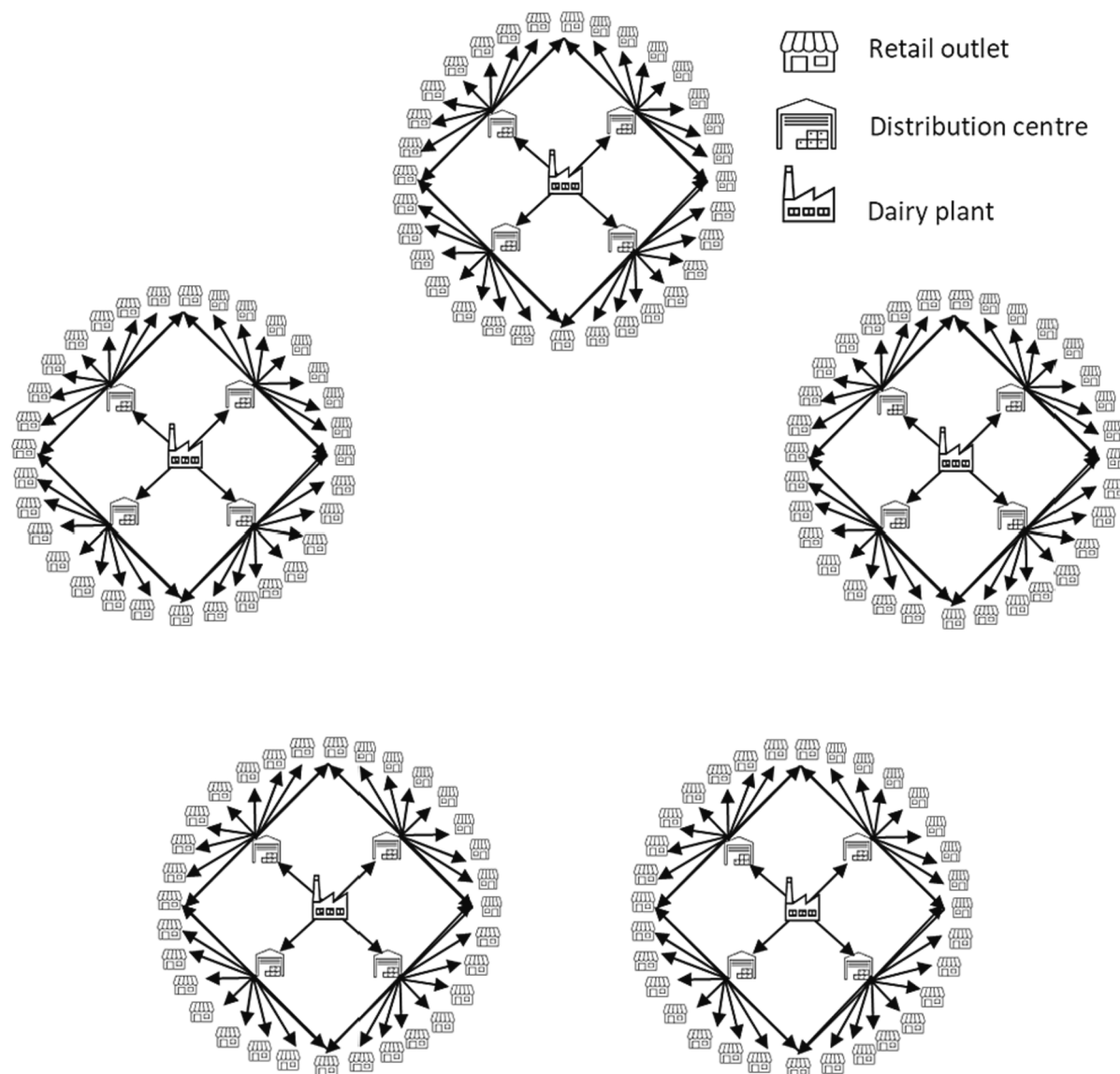


Fig. 7. Schematic of a decentralised milk and cream production system.

Table 6

Codification of the manufacturing and distribution scenarios simulated. The letters acronyms of column 1 are presented in Fig. 5.

Scenario Name	Fuel used for heating needs in manufacturing	Type of refrigerated vehicles	Type of distribution system
ODC	Oil	Diesel	Centralised
GDC	Natural Gas	Diesel	Centralised
HDC	Hydrogen	Diesel	Centralised
OEC	Oil	Electric	Centralised
GEC	Natural Gas	Electric	Centralised
HEC	Hydrogen	Electric	Centralised
ODD	Oil	Diesel	Decentralised
GDD	Natural Gas	Diesel	Decentralised
HDD	Hydrogen	Diesel	Decentralised
OED	Oil	Electric	Decentralised
GED	Natural Gas	Electric	Decentralised
HED	Hydrogen	Electric	Decentralised

10,000 L/h). This is because the model does not account for technological innovations and improved equipment efficiencies, which may be found in large dairy production plants that would improve the energy

performance [25]. In addition, most of the model governing equations have a linear behaviour in different scales.

Driven by the interest in energy mapping of manufacturing and distribution that can allow for identifying energy hotspots, Figs. 8 and 9 offer the share in energy consumption between the different operations taking place. For model validation purposes, literature values for the energy consumption among different operation taking place in milk manufacturing of real processing plants were compared with the respective results of the present study (Fig. 8) and showed great agreement as demonstrated in Table 7 [25]. According to the simulation results in Figs. 8 and 9, the most energy intensive operations for skimmed milk products were 1) product transportation, with a 38% contribution in total product-embodied energy use on average among the scenarios, 2) heat treatment energy requirements in the processing units with a 27% contribution, and 3) the CIP process with a 16% contribution. For cream products, the most energy intensive operations were the 1) heating requirements in processing with a 33% contribution in the total energy use on average, 2) product transportation with a 29% contribution and 3) the CIP process with a 13% contribution. According to this study, these are energy hotspots that the industry should focus on improving their energy performance. The ability of a mechanistic energy consumption model for energy hotspot identification is especially useful

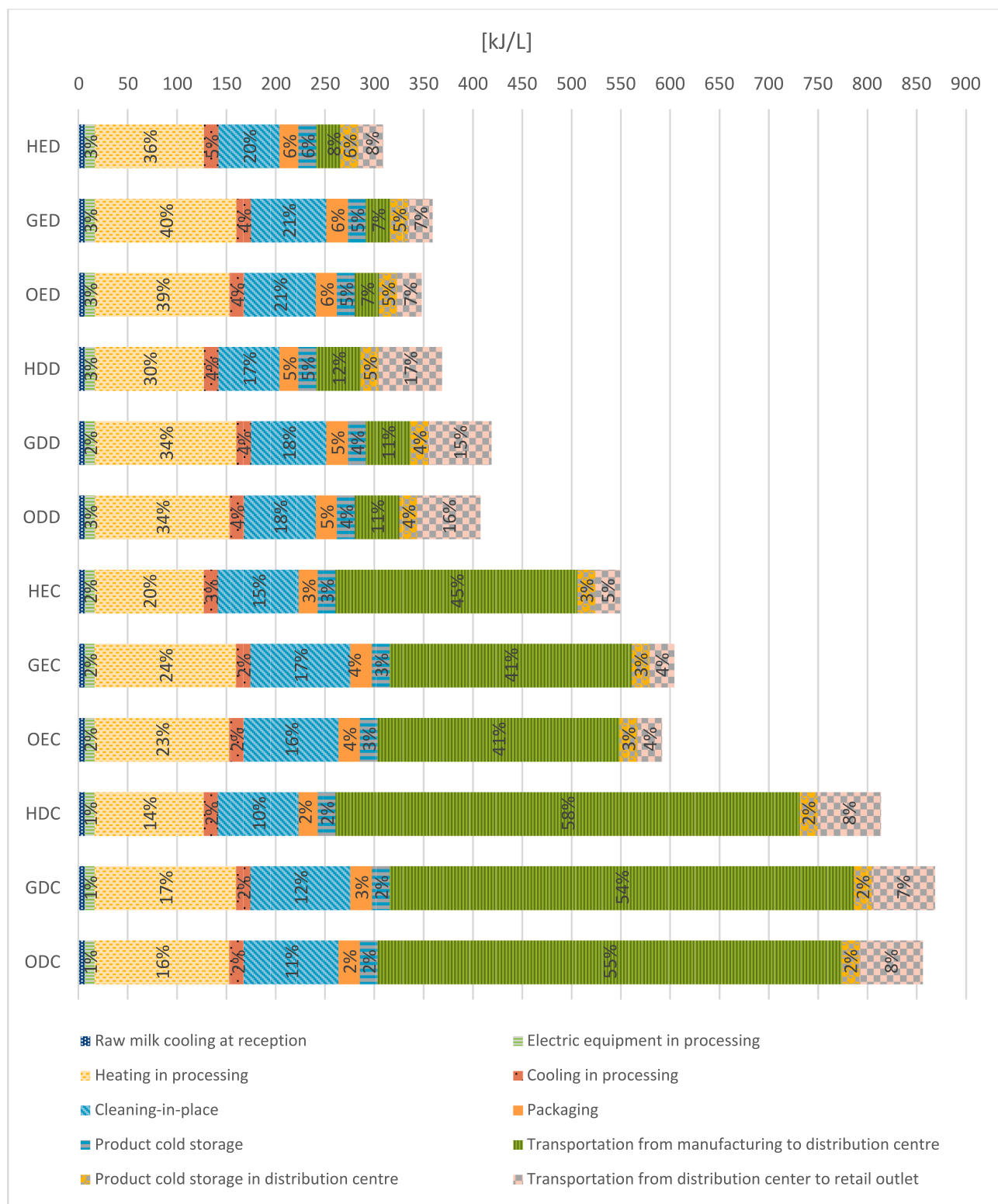


**Fig. 8.** Model simulation results for the energy use for manufacturing and distribution of a unit of skimmed milk product of 1 L [kJ/L] under 12 different manufacturing and distribution scenarios as summarised in Table 6. The figure also presents the share of energy use among different operations taking place in product manufacturing and distribution.

considering that any energy mitigation action usually requires investment at a significant capital cost.

Focusing only on the product-embodied energy for distribution, the results ranged broadly under the 12 different scenarios (Figs. 8 and 9). Specifically, the energy for distribution ranged between 68 and 553 kJ/L

for skimmed milk products and between 22 and 179 kJ/330 ml for cream products (Figs. 8 and 9). The energy demand for decentralised distribution was ~77% less than the energy demand for centralised distribution for both products, which indicates that considering moving towards a decentralised distribution system in the future could lead to

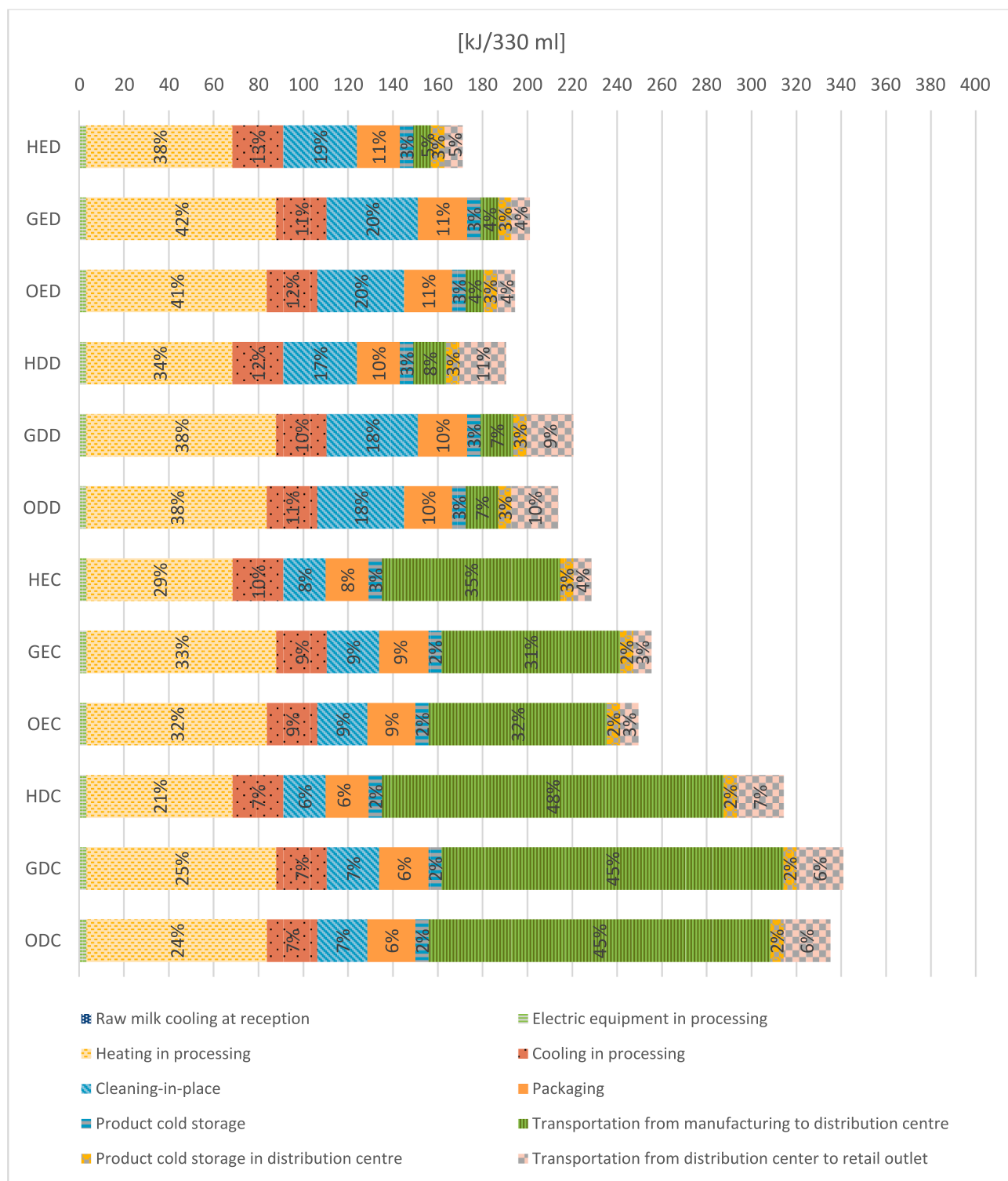


**Fig. 9.** Model simulation results for the energy use for manufacturing and distribution per unit of a 330 ml of cream product measured in [kJ/3030 ml] under 12 different manufacturing and distribution scenarios of dairy manufacturing and distribution as shown in Table 6. The figure also presents the share of energy use among different operations taking place in product manufacturing and distribution.

significant energy savings. However, should be aware that production at the smaller scale might be more energy intensive than at the large scale, thereby counteracting the savings made from the distribution stage. The use of diesel-fuelled refrigerated vehicles for product distribution was around twice as energy intensive as that when electric vehicles were used. According to the simulations, if diesel-fuelled vehicles are replaced with electric ones, this can lead to ~31% energy savings for the

manufacturing and distribution of skimmed milk products and ~26% for cream products, proving that significant energy savings can result from electrifying the distribution stage. The reason why less energy savings is achieved for cream products is because the smaller volume and weight of the product transported, the less energy is required for its transportation, and thus the contribution of the distribution stage is not as significant as for milk products (i.e., the cream packaging is 330 ml

**Table 7**

Comparison of the product embodied energy results presented in Fig. 8 for the share of energy consumption in different operations in manufacturing with average energy breakdown for fluid-milk plants in 1998 in the Netherlands and benchmark value for Canadian plants as presented in the study of Xu & Flapper (2009) [25]. Although the energy in the studies is measured in MJ/kg and the embodied energy in the present study is measured in MJ/L, they are comparable since the density of milk is close to 1.

Stage	Operation	The Netherlands 1998 (primary energy) (MJ/kg)	Canadian benchmark (final energy) (MJ/kg)	This model values (final energy) (MJ/L)		
				Oil	Natural Gas	Hydrogen
Milk reception	<b>Reception/Thermization</b>	0.023	0.018	–		
	<b>Storage</b>	0.076	–	0.065		
Milk treatment	<b>Standardization</b>	0.400	0.018	–		
	<b>Pasteurization*</b>	–	0.189	0.137	0.144	0.111
Packing	<b>Filling/packing</b>	0.090	0.036	0.021	0.022	0.019
Supporting processes	<b>Pressurized air</b>	0.002	–	–		
	<b>CIP</b>	0.100	0.110	0.0963	0.101	0.082
	<b>Cooling</b>	0.200	0.008	0.015		
	<b>refrigeration</b>			0.0181		
	<b>Water provision</b>	0.060	–	–		
	<b>Building/HVAC</b>	0.095	0.0180			
	<b>Other</b>	0.014	0.0310	<b>0.098 (Electrical equipment)</b>		
Total final SEC	(MJ/kg fluid milk)	–	0.43	0.303	0.316	0.261
Total primary SEC	(MJ/kg fluid milk)	1.06	0.68	–		

while milk packaging is 1 L). As a result, for higher density-value products such as cream, a centralised product distribution infrastructure could be more environmentally and financially sustainable.

### 3.2. Energy mapping and carbon footprinting by energy source

Today, manufacturers and suppliers are interested in modelling tools that can quantify the products' carbon footprint in order to assess their products from a sustainability perspective [4,5]. Focusing on the energy-derived carbon footprint for milk and cream, this is not only dependent on the amount of energy consumed, but also on the energy mix of the utilised energy resources. The developed energy consumption model allowed for the quantification of the energy mix used by the different energy resources encompassing electricity, oil or diesel, natural gas, and hydrogen. It also allowed for evaluating the product's carbon footprint from energy use, and the respective share of carbon emission by energy sources. Oil and diesel energy resources were considered together in the results, due to their similarities in their emission factor and calorific value (Table 3, 4).

The simulation results for the energy mix by source (right side) and the corresponding carbon footprint from energy use (left side) are shown in Figs. 10 and 11 for skimmed milk and cream products respectively. The carbon footprint from energy use ranged between 7.6–59.1 g CO<sub>2</sub>e for skimmed milk and 4.4–22.2 g CO<sub>2</sub>e for cream. These results broadly agree in scale with carbon footprint values identified in several LCA studies. In one LCA study, 50 g CO<sub>2</sub>e per L of skimmed milk were allocated for manufacturing and 70 g CO<sub>2</sub>e for transportation, whilst for 0.5 kg of cream about 50 g CO<sub>2</sub>e were allocated for cream processing and 110 g CO<sub>2</sub>e for transportation [85]. Another LCA study allocated 86 g CO<sub>2</sub>e per L of milk for product processing excluding packaging, and 31 g CO<sub>2</sub>e per L of milk for transportation [86]. The lower boundaries of the results from the present study correspond to the “greenest” scenarios, which currently do not exist and no studies in the literature have attempted to provide values for these scenarios to date. In addition, this study accounts only for the energy-derived carbon emissions and not for GHG emissions resulting from other resources.

When considering the energy use by source (Figs. 10 and 11, right side), it can be observed that the product-embodied energy only varies by ±5% in the use of different combustion fuels for manufacturing heating needs (eg. ODC vs GDC vs HDC). These slight differences are due to differences in the efficiency of different fuel combustion technologies

between oil natural gas, and hydrogen burning boilers [67,68]. However, since the different fuel used have a significant difference in their emission factor, the corresponding differences in carbon emissions (left side in Figs. 10 and 11) are therefore more significant. The scenarios where natural gas is used instead of oil were 6–14% less emitting, irrespective of the product considered. Whilst in those scenarios where hydrogen is used, these were 30–63% less emitting compared to oil usage.

### 3.3. Projections of dairy manufacturing and distribution carbon emissions towards 2050

As with every industry, dairy manufacturing and distribution needs to meet the net zero carbon target by 2050. Today, industry bodies are especially interested in modelling tools that can project the evolution of their system's carbon footprint towards 2050, subsequent to energy mitigation decisions. This could facilitate the identification of an optimal roadmap towards net zero, including one that adapts to emerging alternative technologies and/or evolving industry behaviours and attitudes. The developed energy consumption model allows for the projection of the carbon footprint of the manufacturing and distribution system towards 2050. To project the evolution of the carbon emission for the studied scenarios summarised in Table 6, the expected gradual reduction of the emission factor for electricity as a result of the electricity decarbonisation for the UK was taken into account [67]. The annual energy use carbon footprint projections for the simulated scenarios are presented in Fig. 12. All scenarios are equivalent in terms of production capacity and as a result are comparable with each other as explained in Section 2.5.

Fig. 12 indicates the reduction rate of the energy related carbon emissions of the simulated scenarios accounting for the UK's electricity decarbonisation targets from 2020 to 2050. It can be observed that the higher the electricity rate in the energy mix for each scenario (see Figs. 10 and 11), the greater the emissions savings that can be achieved. For example, scenario GED (in Fig. 12) can lead to 21.1% emissions reductions by 2050, versus 2020 levels. For several scenarios, the emission reduction rate from 2020 to 2050 does not appear in Fig. 12. This is because those scenarios could not realistically exist in 2020, due to the unavailability of the simulated technology at a commercial scale. Specifically, the use of green hydrogen for the manufacturing heating needs in 2020 could not exist, leading to the exclusion of scenarios HDC,

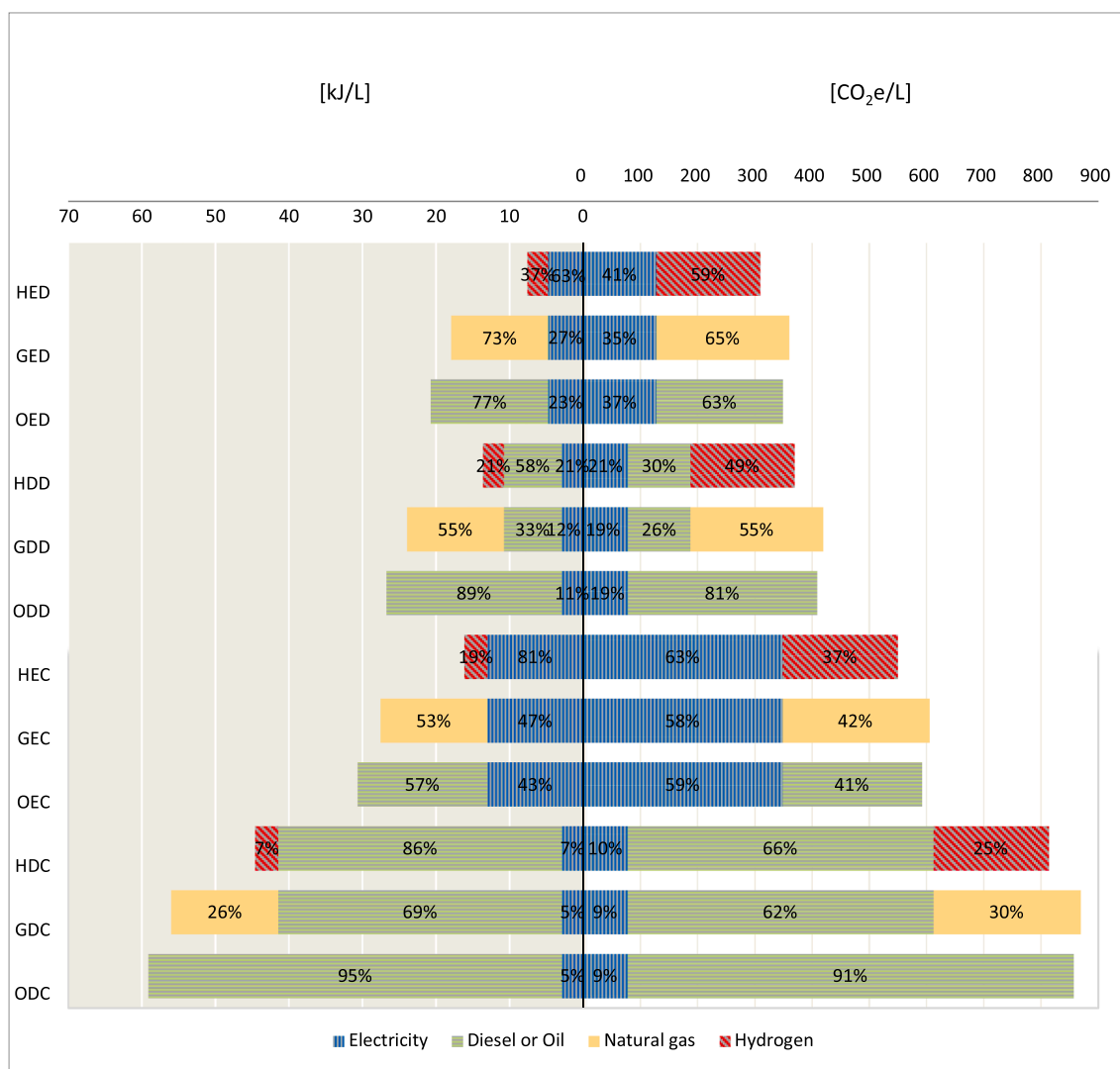


**Fig. 10.** Energy use [kJ] (right side) and emissions from energy use [CO<sub>2</sub>e] (left side) per L of skimmed milk manufacturing and distribution for the year 2020 under 12 scenarios of Table 6. The figure also presents the energy mix between the different energy resources used in each scenario.

HEC, HDD and HED. Also, there were insufficient electricity charging points in the UK in 2020 which negates long-haul requirements for a centralised distribution system, which leads to the exclusion of scenarios OEC, GEC, and HEC. The resulting reduction rates for the realistic scenarios in Fig. 12 (Scenarios ODC, GDC, ODD, GDD, OED and GED) clearly indicate that dairy companies cannot expect to reach the net zero carbon target just by relying on Government electricity decarbonisation planning to facilitate their dairy manufacturing and distribution system to the net zero carbon levels by 2050. Subsequent to reaching the appropriate technology readiness level (TRL) as the years pass, those technologies that will then become commercially available and merge onto the market, would allow moving from scenario to scenario and ever greener outcomes (subject to industry appetite with implementing new technology). Thus, dairy companies should carefully consider which net zero carbon practices to apply, in order to meet the net zero carbon targets.

For the dairy sector to achieve net zero emissions from manufacturing and distribution by 2050, a range of interventions are required as no individual action alone would achieve the required net zero target. Fig. 13 presents the same results of Fig. 12, but this time the results provide an example of a possible roadmap towards net zero by 2050. As a roadmap starting point, it is assumed that the studied manufacturing and distribution system was represented by scenario

ODC which realistically existed in 2020. If by 2030, oil burning boilers can be replaced with natural gas boilers, the system will be represented by the GDC scenario in 2030, leading to an 7.6% emissions reduction versus the 2020 levels. Then, if by 2040 the diesel refrigerated vehicles are replaced with electric powered vehicles, the system in 2040 will be represented by the GEC scenario and a 37.1% emissions reduction will be achieved (when compared to 2020 levels). Finally, if by 2050, the natural gas boilers are replaced by hydrogen ones, and thus moving to scenario HEC, a 90.2% emissions reduction will be achieved when compared to the 2020 levels. Overall, by following the recommended roadmap and gradually transitioning from the ODC scenario in 2020 to the HEC scenario in 2050, the carbon emissions from energy use can be reduced by 90.2%. It is worth noting that the example used as a possible roadmap for moving towards net zero (Fig. 13) is not the only possible one, but different routes could be followed. This also demonstrates the adaptiveness of the model and resulting roadmap in response to evolving technology and industry attitudes. The roadmap path to be chosen is for decision makers, and responsive to government regulations and TRLs/take up. The emission quantification and roadmap planning visualisation capability that the model offers is a further benefit to aid decision making and communication to multi-disciplines audiences within and between sites and sectors.



**Fig. 11.** Energy use [kJ] (right side) and emissions from energy use [CO<sub>2</sub>e] (left side) per 330 ml of cream manufacturing and distribution in 2020 under 12 scenarios of Table 6. The figure also presents the energy mix between the different energy resources used in each scenario.

#### 4. Conclusion

Global companies are facing an existential threat in view of climate change and must act now to reduce their carbon footprint. In order to drive carbon emissions reductions, detailed roadmaps are required covering the whole supply chain and for periods of time that align to 2050 targets. Modelling is a useful cost and time effective way to inform and support on decision making in changing technological landscapes such as the food industry. This study presents a novel methodology for conducting a mechanistic end-to-end model of a dairy manufacturing and distribution chain. The presented model allows for the evaluation of energy use and related carbon emissions for the manufacturing and distribution of milk and cream products. The mechanistic modelling approach provides simulation flexibility under different scales of production and energy resources utilised, and therefore 12 ranging scenarios were simulated. The product-embodied energy and carbon footprint for 1 L skimmed milk products ranged between 309 and 869 kJ/L and between 7.6 and 59.1 g CO<sub>2</sub>e/L, depending on the simulated scenario. The respective values for 330 ml cream products, ranged between 173 and 343 kJ and 4.4 to 22.6 g CO<sub>2</sub>e. The most energy intensive operations for both products were transportation, the CIP process, and heat treatment. The scenarios were also simulated towards 2050 to demonstrate the relevance of the model to the current food industry

targets and show how it could be applied to produce a detailed and realistic roadmap for hitting the net zero target. The results demonstrated that the 2050 net zero target cannot be realised by following government-mandated targets alone. Instead, the results illustrated that with step-by-step changes that move from scenario to scenario over time and availability, this could deliver up to 90.2% carbon-emission reductions by 2050 (when compared to 2020 levels).

This model is a promising decision-making tool for the dairy and the broader food sector, which can be justified by the following model capabilities. First, it allows for energy mapping of the manufacturing and distribution operations of existing systems. This reveals the energy hotspots, which should be primarily targeted for energy and emission mitigation actions. The model's flexibility allows for accommodating various energy sources or distribution methods that can arise in the future and allows for assessing alternative energy mitigation actions before implementation. In addition, the model is adaptive, meaning that as "cleaner greener" fuels and/or alternative food processing technologies become available, and as consumer demand and preferences shift, these changes can be incorporated into the model. The advantage of the presented modelling methodology is that it can guide the development of approaches to reach net zero carbon emissions across the wider food and drink industry and into other industries. Overall, the model can quantitatively and visually aid roadmap planning towards the net zero

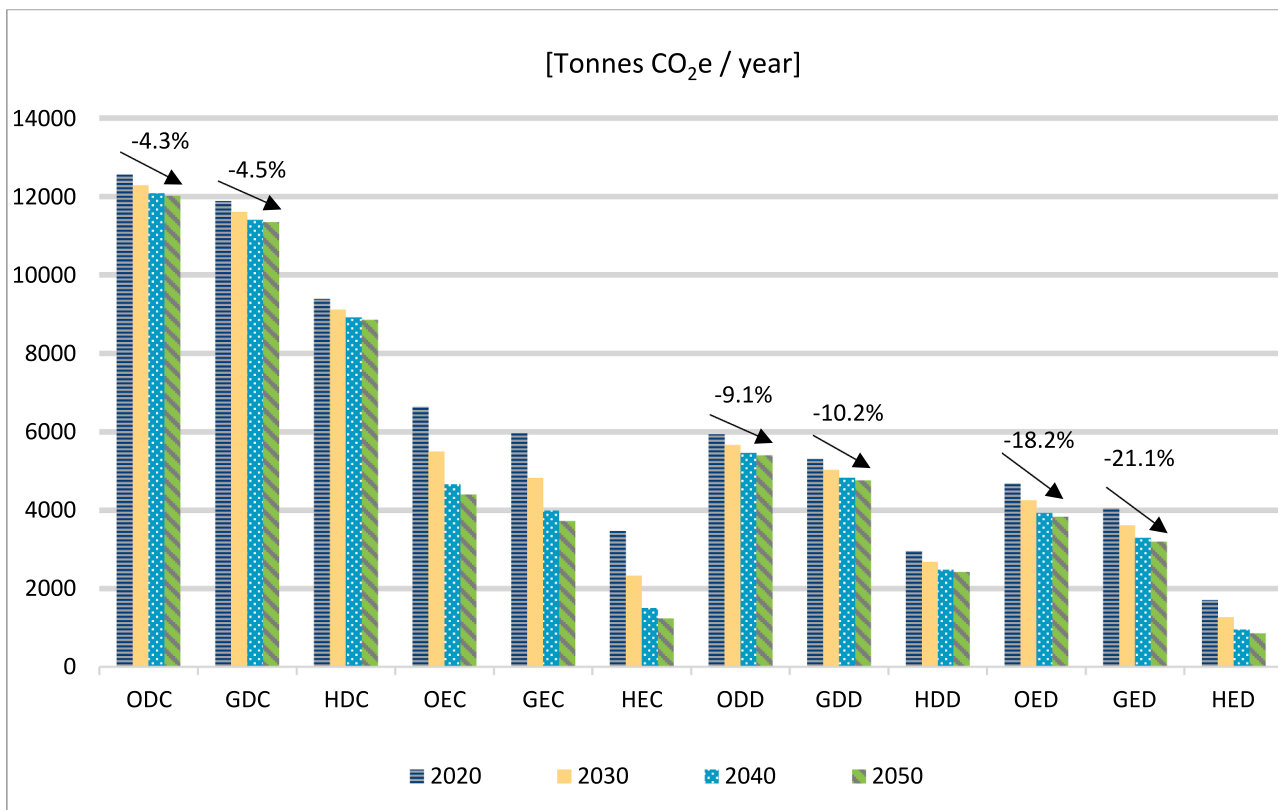


**Fig. 12.** Annual carbon footprint per manufacturing and distribution scenario in the start of each decade (2020 – 2050) [Tonnes CO<sub>2</sub>e/year]. The figure indicates with arrows the emissions reductions towards 2050 for several manufacturing & distribution scenarios [Tonnes CO<sub>2</sub>e/year]. The emission reductions are indicated only in scenarios ODC, GDC, ODD, GDD, OED and GED, since these are the only realistic scenarios that could be realistically existing in 2020.

carbon target by 2050, which is a substantial need for businesses and stakeholders today.

#### CRedit authorship contribution statement

**Maria Ioanna Malliaroudaki:** Conceptualization, Methodology, Software, Validation, Formal analysis, Investigation, Data curation, Writing – original draft, Writing – review & editing, Visualization. **Nicholas J. Watson:** Writing – review & editing, Supervision. **Zachary J. Glover:** Writing – review & editing. **Luanga N. Nchiri:** Writing – review & editing. **Rachel L. Gomes:** Conceptualization, Writing – review & editing, Supervision, Project administration, Funding acquisition, Visualization.

#### Symbols

Variable	Description	Equation	Unit
$COP_{comp}$	$COP_{comp}$ is the coefficient of performance (COP) of the compressor of the refrigeration system	31, 32	–
$\dot{Q}_{cf,n}$	Heating energy required to heat the cleaning fluid of the step $n$ of the CIP cycle	14, 15	$\frac{kJ}{s}$
$C_{ph}$	Specific heat capacity at constant pressure of the hot side stream of the heat exchanger	8	$\frac{kJ}{kgK}$
$C_{pc}$	Specific heat capacity at constant pressure of the cold side stream of the heat exchanger	8	$\frac{kJ}{kgK}$
$C_{p,cf}$	Specific heat capacity at constant pressure of the cleaning fluid	14	$\frac{kJ}{kgK}$

(continued on next column)

(continued)

Variable	Description	Equation	Unit
$C_p$	Specific heat capacity at constant pressure of a stream passing through a heat exchanger	6, 7	$\frac{kJ}{kgK}$
$E_{tr}$	Fuel demand for transportation of a diesel or electric fuelled refrigerated vehicle	34	$kJ$
$E_{red}$	Electrical energy for refrigeration of a diesel powered refrigerated vehicle	35	$kJ$
$E_{red}$	Electrical energy for refrigeration of an electric powered refrigerated vehicle	36	$kJ$
$\dot{H}_{i,in}$	Enthalpy rate of the inlet stream $i$ of a unit operation	2	$\frac{kJ}{s}$
$\dot{H}_{j,out}$	Enthalpy rate of the outlet stream $i$ of a unit operation	2	$\frac{kJ}{s}$
$\dot{Q}_{exchange}$	Duty exchange rate between the hot and the cold stream side of each heat exchanger	9, 10	$\frac{kJ}{s}$
$\dot{Q}_{net,in}$	Net heat rate input to the system	2, 3	$\frac{kJ}{s}$
$\dot{V}_{pump}$	Volume flow rate of stream entering the pump	26	$\frac{m^3}{s}$
$\dot{W}_{hom}$	Power demand of the homogeniser	30	$\frac{kJ}{s}$
$\dot{W}_{cent}$	Power consumption of the centrifugal separator device	28	$\frac{kJ}{s}$
$\dot{W}_k$	Electrical or fuel power consumption of a continues process	37, 38	$\frac{kJ}{s}$
$\dot{W}_{net,out}$	Net work rate output from system	2, 3	$\frac{kJ}{s}$
$\dot{W}_{pump}$	Electric power consumption of a pump	24, 27	$\frac{kJ}{s}$

(continued on next page)

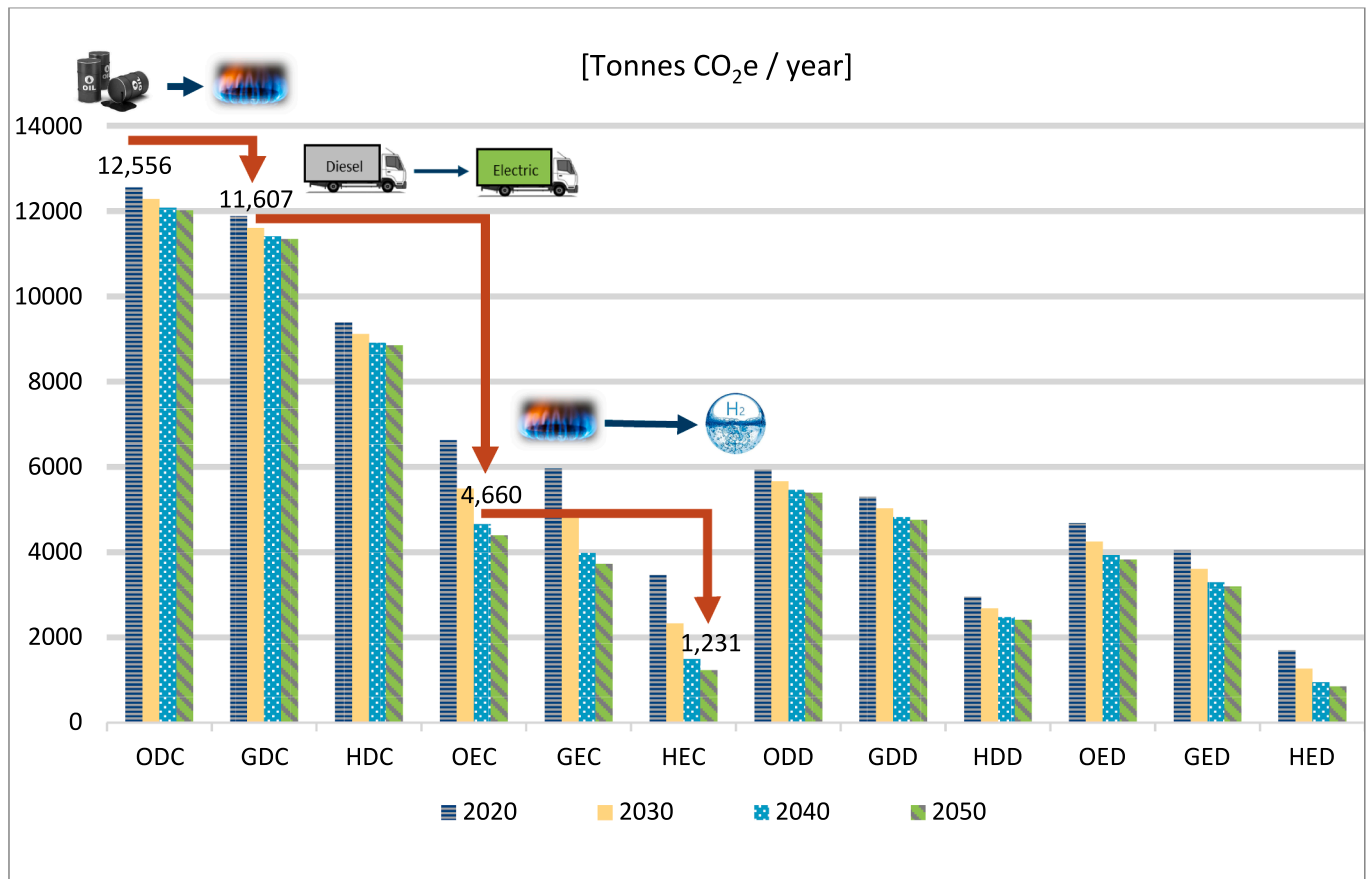


**Fig. 13.** Annual carbon footprint per manufacturing and distribution scenario in the start of each decade (2020 – 2050) [Tonnes CO<sub>2</sub>e/year]. The figure indicates roadmap towards net-zero by 2050, moving from scenario to scenario every decade, from 2020 to 2050. [Tonnes CO<sub>2</sub>e/year].

(continued)

Variable	Description	Equation	Unit
$\dot{W}_{sep,pump}$	Power consumption of the pump of the centrifugal separator	28, 29	$\frac{kJ}{s}$
$\dot{W}_{tot,sep}$	Overall power consumption of the centrifugal separator	28	$\frac{kJ}{s}$
$\dot{a}_k$	Rate of mass that is treated through the process or equipment $k$	37, 38	$\frac{kg}{s}$
$\dot{m}_h$	Mass flow rate of the hot side stream of the heat exchanger	8	$\frac{kg}{s}$
$\dot{m}_{hom}$	Mass flow rate of the inlet stream to the homogeniser	30	$\frac{kg}{s}$
$\dot{m}_c$	Mass flow rate of the cold side stream of the heat exchanger	8	$\frac{kg}{s}$
$\dot{m}_{c,out}$	Mass flow rate of cream stream exiting the separator	4, 5	$\frac{kg}{s}$
$\dot{m}_{cf}$	Mass flowrate of the cleaning fluid	13, 14	$\frac{kg}{s}$
$\dot{m}_{i,in}$	Mass flow rates of the inlet stream $i$ to a unit operation	1, 3	$\frac{kg}{s}$
$\dot{m}_{j,out}$	Mass flow rates of the outlet stream $j$ to a unit operation	1, 3	$\frac{kg}{s}$
$\dot{m}_{pump}$	Mass flow rate of the stream that enters the pump	24	$\frac{kg}{s}$
$\dot{m}_{sep}$	Mass flow rate of the inlet stream of the centrifugal separator	29	$\frac{kg}{s}$
$\dot{m}_{sm,out}$	Mass flow rate of skimmed milk stream exiting the separator	4, 5	$\frac{kg}{s}$
$\dot{m}_{wm,in}$	Mass flow rate of whole milk stream entering the separator	4, 5	$\frac{kg}{s}$
$t_{cf,n}$	Time of cleaning of the cleaning step $n$	15	$s$
$ \Delta P_{hom} $	Pressure rise resulted by the stream passing through the homogeniser	30	$Pa$

(continued on next column)

(continued)

Variable	Description	Equation	Unit
$ \Delta P_{pump} $	Absolute pressure rise through the pump	25	$Pa$
$ \Delta P_{sep} $	Pressure rise of the pump in the centrifugal separator	29	$Pa$
$h_{i,in}$	Specific enthalpy of the inlet stream $i$ of a unit operation	3, 6, 7	$\frac{kJ}{kg}$
$h_{j,out}$	Specific enthalpy of the outlet stream $j$ of a unit operation	3, 6, 7	$\frac{kJ}{kg}$
$\Delta P_p$	pressure drop due to flow in the pipeline	18	
$A_{he}$	Heat exchange surface of the plate heat exchanger	10, 11	$m^2$
$A_{en}$	heat exchange surface of the enclosure	23	$m^2$
$A_{pt}$	Surface area of a plate of the plate heat exchanger	11	$m^2$
$A_{tw}$	Heat exchange surface of the cooling tank	21	$m^2$
$C_{pm}$	Specific heat capacity of raw milk stored	20	$\frac{kJ}{kgK}$
$CF_{system}$	Annual carbon footprint of total skimmed milk and cream manufacturing and distribution system	39	$\frac{tonnes CO_2e}{year}$
$CF_{unit}$	Product's carbon footprint	38	$kg CO_2e$
$CV_k$	gross calorific value of the used fuel or electricity for the process $k$	37, 38	$\frac{kJ}{kWh}$ or $\frac{kJ}{kg}$ or $\frac{kJ}{L}$
$E_{cf}$	electrical energy required to power the refrigeration system	31	$kJ$
$E_i$	Benchmarking value for the energy intensity per unit of distance and mass of load	34	$kJ$

(continued on next page)

(continued)

Variable	Description	Equation	Unit
$E_k$	Energy consumption of an operation or process k	37, 38	$kJ$
$E_{tr}$	Energy for transportation of a refrigerated vehicle	33	$kJ$
$E_{re}$	Energy for refrigeration of a refrigerated vehicle	33	$kJ$
$E_{rv}$	Total diesel- or electric-energy consumed by a refrigerated vehicle	33	$kJ$
$E_{unit}$	Product-embodied energy	37	$kJ$
$F_{c,out}$	Fat content (w/w %) of the skimmed milk stream exiting the separator	5	$\frac{kg}{kg}$
$F_{sm,out}$	Fat content (w/w %) of the skimmed milk stream exiting the separator	5	$\frac{kg}{kg}$
$F_{wm,in}$	Fat is the fat content (w/w %) of the whole milk stream entering the separator	5	$\frac{kg}{kg}$
$H_{pump}$	Total head of pump	24, 25, 26	$m$
$N_{pt}$	Number of plates of the plate heat exchanger	11	–
$Q_{T,ct}$	Thermal load on the cooling tank	19	$kJ$
$Q_{T,SC}$	Thermal load on the cold storing chamber	22	$kJ$
$Q_T$	Thermal Load on a cooling facility	31	$kJ$
$Q_{cleaning}$	Total heating energy required for cleaning	15	$kJ$
$Q_{do}$	Heat losses due to door openings of the cold storing chamber	22	$kJ$
$Q_{ele}$	Heat released by electrical equipment such as light bulbs and circulation air fans	22	$kJ$
$Q_{en}$	Heat transmission through the enclosures of the cold storing chamber	22, 23	$kJ$
$Q_{pe}$	Heat losses due to due to people entering the storage chamber	22	$kJ$
$Q_{pr}$	Heat released during products' cooling in the cold storing chamber	22	$kJ$
$Q_{rmc}$	Heat released during raw milk's cooling	19, 20	$kJ$
$Q_{rw}$	Heat transmission through the tank walls	19, 21	$kJ$
$R_e$	Reynolds number in the pipeline	16	
$T_{h,in}$	Inlet temperature of the hot side stream of the heat exchanger	8	$^{\circ}C$
$T_{h,out}$	Outlet temperature of the hot side stream of the heat exchanger	8	$^{\circ}C$
$T_{amb}$	Ambient temperature	21	$^{\circ}C$
$T_{c,out}$	Outlet temperature of the cold side stream of the heat exchanger	8	$^{\circ}C$
$T_{c,in}$	Inlet temperature of the cold side stream of the heat exchanger	8	$^{\circ}C$
$T_{cf,amb}$	Initial cleaning fluid temperature	14	$^{\circ}C$
$T_{cf}$	Temperature of the cleaning fluid for the cleaning step $n$	14	$^{\circ}C$
$T_{cond}$	average temperature of the condenser of the refrigeration system	32	$^{\circ}C$
$T_{cs}$	Cold-storing temperature of the cooling tank	20	$^{\circ}C$
$T_{evap}$	Average temperature of the evaporator of the refrigeration system	32	$^{\circ}C$
$T_{in}$	Inlet temperature of one side's stream of a heat exchanger	6, 7	$^{\circ}C$
$T_{jout}$	Outlet temperature of one side's stream of a heat exchanger	6, 7	$^{\circ}C$
$T_{pr}$	Storing temperature of products in the cold storing chamber	23	$^{\circ}C$
$T_{rm,i}$	Initial temperature of raw milk loaded in the cooling tank	20	$^{\circ}C$
$U_{he}$	Overall heat transfer coefficient of the plate heat exchanger	10	$\frac{W}{m^2K}$

(continued on next column)

(continued)

Variable	Description	Equation	Unit
$U_{en}$	Overall heat transfer coefficient of the chamber or refrigeration unit enclosures	23	$\frac{W}{m^2K}$
$U_{tw}$	Overall heat transfer coefficient for the tank wall	21	$\frac{W}{m^2K}$
$\dot{V}$	Volume flowrate of stream in the pipeline	12	$\frac{gal}{min}$
$d_{id}$	Ideal pipeline diameter	12	$in$
$d_{st}$	Standardised pipeline diameter	13	$m$
$f_c$	Emission factor or Carbon conversion factor of a fuel or electricity	38	$\frac{kg\ CO_2e}{kWh}$ or $\frac{kg\ CO_2e}{kg\ of\ fuel}$
$f_p$	friction factor of the pipeline	16	
$m_k$	total product mass treated through the process or operation $k$	37, 38	$kg$
$m_p$	mass load of product transported	34	$tonne$
$m_{rm}$	Total mass of raw milk in the cooling tank	20	$kg$
$m_{unit}$	mass of a product unit	37, 38	$kg$
$n_{tot,C}$	Total number of cream products manufactured annually	39	–
$n_{tot,SM}$	Total number of skimmed milk products manufactured annually	39	–
$u_{cf}$	Cleaning fluid velocity in the pipeline	13	$\frac{m}{s}$
$\Delta h$	The difference of the specific enthalpy between the inlet and the outlet of a stream	4, 5	
$\Delta h_{vap}$	Latent heat of vaporization of the stream $i$	4, 5	$\frac{kJ}{kg}$
$\eta_{hom}$	Pump efficiency of the homogeniser	30	–
$\eta_{h,el,mot}$	Electric motor efficiency of the homogeniser	30	–
$\eta_{ge}$	Efficiency of the electric generator of a diesel powered refrigerated vehicle	35	–
$\eta_{pump,sep}$	pump efficiency of the centrifugal separator	29	–
$\eta_{pump}$	Centrifugal pump efficiency	24, 26	–
$\eta_{p,el,mot}$	Electric motor efficiency of centrifugal pump	24, 27	–
$\eta_{mc}$	Efficiency of the motor of the compressor of a refrigeration facility	31	–
$\eta_{DC-DC}$	Efficiency of DC-DC converter in electric vehicles	36	–
$\eta_{charging}$	Efficiency of battery charging from grid electricity in electric vehicles	36	–
$\rho_{cf}$	Density of the cleaning fluid	13	$\frac{kg}{m^3}$
$\rho_{pump}$	Density of the pumped fluid	25	$\frac{kg}{m^3}$
$L$	Length of the pipeline	18	$m$
$d$	Transportation distance of a route	34	$km$
$g$	gravity acceleration	24, 25	$\frac{m}{s^2}$
$i$	Stream entering a unit operation	1, 2, 3	–
$j$	Stream exiting a unit operation	1, 2, 3	–
$k$	Number indicator for a process unit or an equipment	37, 38	–
$n$	Cleaning step numbering	14, 15	
$u$	fluid velocity	17, 18	$\frac{m}{s}$
$\Delta \dot{H}$	Difference in enthalpy rate between the inlet and outlet stream from one side of a heat exchanger	9	$\frac{kJ}{s}$
$\mu$	fluid dynamic viscosity	17	$Pa\ s$
$\rho$	Density of fluid	17, 18	$\frac{kg}{m^3}$

### Declaration of Competing Interest

The authors declare that they have no known competing financial interests or personal relationships that could have appeared to influence the work reported in this paper.

## Data availability

The authors have used data from the referenced studies

## Acknowledgements

The authors would like to acknowledge Arla Foods Ltd, UK and NIZO, the Netherlands for their industry-specific advice and operational information that supported this work.

## Funding

This project is part of the PROTECT ITN (<http://www.protect-itn.eu/>) which is funded under the European Union's Horizon 2020 research and innovation programme under the Marie Skłodowska-Curie grant agreement No. 813329.

## Appendix A. Supplementary data

Supplementary data to this article can be found online at <https://doi.org/10.1016/j.cej.2023.145734>.

## References

- [1] Food and Agriculture Organization of the United Nations, ed. The future of food and agriculture: trends and challenges, Food and Agriculture Organization of the United Nations, Rome. 2017.
- [2] Joint Research Centre (European Commission), P. Bertoldi, B. Notarnicola, F. Monforti-Ferrario, P. Renzulli, S. Sala, E. Saouter, H. Medarac, D. Pennington, V. Motola, G. Tassielli, N. Labanca, I. Pinedo Pascua, L. Castellazzi, J.-F. Dallemand, M. Banja, M. Goralczyk, N. Scarlat, E.M. Schau, Energy use in the EU food sector: state of play and opportunities for improvement, Publications Office of the European Union, LU, 2015 accessed April 5, 2023.
- [3] FAO. "Energy-smart" food for people and climate: issue paper, Food and Agriculture Organization of the United Nations, Rome, Italy, 2011. <https://www.fao.org/3/i2454e/i2454e.pdf>.
- [4] A. Ladha-Sabur, S. Bakalis, P.J. Fryer, E. Lopez-Quiroga, Mapping energy consumption in food manufacturing, Trends in Food Science & Technology. 86 (2019) 270–280, <https://doi.org/10.1016/j.tifs.2019.02.034>.
- [5] S. Gerosa, J. Skoet, eds., Milk availability: trends in production and demand and medium-term outlook, 2012. <https://doi.org/10.22004/ag.econ.289000>.
- [6] S.A. Rankin, R.L. Bradley, G. Miller, K.B. Mildenhall, A 100-Year Review: A century of dairy processing advancements—Pasteurization, cleaning and sanitation, and sanitary equipment design, Journal of Dairy Science. 100 (2017) 9903–9915, <https://doi.org/10.3168/jds.2017-13187>.
- [7] S.J. Rad, M.J. Lewis, Water utilisation, energy utilisation and waste water management in the dairy industry: A review, International Journal of Dairy Technology. 67 (2014) 1–20, <https://doi.org/10.1111/1471-0307.12096>.
- [8] R.J. Feliciano, P. Guzmán-Luna, G. Boué, M. Mauricio-Iglesias, A. Hospido, J.-M. Membré, Strategies to mitigate food safety risk while minimizing environmental impacts in the era of climate change, Trends in Food Science & Technology. 126 (2022) 180–191, <https://doi.org/10.1016/j.tifs.2022.02.027>.
- [9] N. Alexandratos, World Agriculture towards 2030/2050: the 2012 revision, (2012).
- [10] M.I. Malliaroudaki, N.J. Watson, R. Ferrari, L.N. Nchari, R.L. Gomes, Energy management for a net zero dairy supply chain under climate change, Trends in Food Science & Technology. 126 (2022) 153–167, <https://doi.org/10.1016/j.tifs.2022.01.015>.
- [11] G. Thoma, J. Popp, D. Nutter, D. Shonnard, R. Ulrich, M. Matlock, D.S. Kim, Z. Neiderman, N. Kemper, C. East, F. Adom, Greenhouse gas emissions from milk production and consumption in the United States: A cradle-to-grave life cycle assessment circa 2008, International Dairy Journal. 31 (2013) S3–S14, <https://doi.org/10.1016/j.idairyj.2012.08.013>.
- [12] C.G.F. Bataille, Physical and policy pathways to net-zero emissions industry, WIREs Climate Change. 11 (2020) e633.
- [13] IPCC, Global Warming of 1.5°C: IPCC Special Report on Impacts of Global Warming of 1.5°C above Pre-industrial Levels in Context of Strengthening Response to Climate Change, Sustainable Development, and Efforts to Eradicate Poverty, 1st ed., Cambridge University Press, 2018. <https://doi.org/10.1017/9781009157940>.
- [14] Page not found, FoodDrinkEurope. (n.d.). [https://www.fooddrinkeurope.eu/wp-content/uploads/2021/09/Decarbonising-the-European-food-and-drink-manufacturing-sector\\_v2.pdf%20Accessed](https://www.fooddrinkeurope.eu/wp-content/uploads/2021/09/Decarbonising-the-European-food-and-drink-manufacturing-sector_v2.pdf%20Accessed) (accessed April 5, 2023).
- [15] I. Cameron, A. Lopez, A. Yule, Decarbonisation road map for the European food and drink manufacturing sector, FoodDrinkEurope, , Fermi Avenue, Harwell, Didcot, OX11 0QR, UK, 2021. [https://www.fooddrinkeurope.eu/wp-content/uploads/2021/09/Decarbonising-the-European-food-and-drink-manufacturing-sector\\_v2.pdf](https://www.fooddrinkeurope.eu/wp-content/uploads/2021/09/Decarbonising-the-European-food-and-drink-manufacturing-sector_v2.pdf).
- [16] The Dairy Roadmap, 2018. [https://www.dairyuk.org/publications/the-dairy-roadmap/\(accessed April 5, 2023\)](https://www.dairyuk.org/publications/the-dairy-roadmap/(accessed April 5, 2023)).
- [17] A. Millot, A. Krook-Riekkola, N. Maizi, Guiding the future energy transition to net-zero emissions: Lessons from exploring the differences between France and Sweden, Energy Policy 139 (2020), 111358, <https://doi.org/10.1016/j.enpol.2020.111358>.
- [18] J. Atuonwu, S. Tassou, Decarbonisation of food manufacturing by the electrification of heat: A review of developments, technology options and future directions, Trends in Food Science & Technology. 107 (2021) 168–182, <https://doi.org/10.1016/j.tifs.2020.10.011>.
- [19] G. Ramkumar, B. Arthi, S.D.S. Jebaseelan, M. Gopila, P. Bhuvanewari, R. Radhika, G.G. Kailo, D. Barik, Implementation of Solar Heat Energy and Adsorption Cooling Mechanism for Milk Pasteurization Application, Adsorption Science & Technology. 2022 (2022) 1–13, <https://doi.org/10.1155/2022/5125931>.
- [20] S. van Renssen, The hydrogen solution? Nature Climate Change 10 (2020) 799–801, <https://doi.org/10.1038/s41558-020-0891-0>.
- [21] P.M. Falcone, M. Hieta, A. Sapio, Hydrogen economy and sustainable development goals: Review and policy insights, Current Opinion in Green and Sustainable Chemistry. 31 (2021), 100506, <https://doi.org/10.1016/j.cogsc.2021.100506>.
- [22] F. Dawood, M. Anda, G.M. Shafiuallah, Hydrogen production for energy: An overview, International Journal of Hydrogen Energy. 45 (2020) 3847–3869, <https://doi.org/10.1016/j.ijhydene.2019.12.059>.
- [23] M. Hermesmann, T.E. Müller, Green, Turquoise, Blue, or Grey? Environmentally friendly Hydrogen Production in Transforming Energy Systems, Progress in Energy and Combustion Science 90 (2022), 100996, <https://doi.org/10.1016/j.peccs.2022.100996>.
- [24] S. Liaros, Circular Food Futures: What Will They Look Like? Circ. Econ. Sust. 1 (2021) 1193–1206, <https://doi.org/10.1007/s43615-021-00082-5>.
- [25] T. Xu, J. Flapper, Energy use and implications for efficiency strategies in global fluid-milk processing industry, Energy Policy 37 (2009) 5334–5341, <https://doi.org/10.1016/j.enpol.2009.07.056>.
- [26] A. Almena, E. Lopez-Quiroga, P.J. Fryer, S. Bakalis, Towards the decentralisation of food manufacture: effect of scale production on economics, carbon footprint and energy demand, Energy Procedia 161 (2019) 182–189, <https://doi.org/10.1016/j.egypro.2019.02.080>.
- [27] [WORLDKINGS DISCOVERY] P10. Mudanjiang City Mega Farm (China): The World's biggest dairy farm., Worldkings - World Records Union. (n.d.). <https://worldkings.org/443/news/new-nominations/world-discovery-p10-mudanjiang-city-mega-farm-china-the-worlds-biggest-dairy-farm> (accessed April 5, 2023).
- [28] dairyreporter.com, Arla Foods UK to officially open 'world's largest' fresh milk plant, Dairyreporter.Com. (2014). <https://www.dairyreporter.com/Article/2014/05/28/Arla-Foods-UK-to-officially-open-world-s-largest-fresh-milk-plant> (accessed April 5, 2023).
- [29] P. Gimenez-Escalante, S. Rahimifard, Challenges in Implementation of a Distributed and Localised Approach to Food Manufacturing, Food Studies: An Interdisciplinary Journal. 8 (2018) 1–14. <https://doi.org/10.18848/2160-1933/CGP/v08i03/1-14>.
- [30] S. Pye, O. Broad, C. Bataille, P. Brockway, H.E. Daly, R. Freeman, A. Gambhir, O. Geden, F. Rogan, S. Sanghvi, J. Tomei, I. Vorushylo, J. Watson, Modelling net-zero emissions energy systems requires a change in approach, Climate Policy. 21 (2021) 222–231, <https://doi.org/10.1080/14693062.2020.1824891>.
- [31] N. Yakovleva, J. Sarkis, T. Sloan, Sustainable benchmarking of supply chains: the case of the food industry, International Journal of Production Research. 50 (2012) 1297–1317, <https://doi.org/10.1080/00207543.2011.571926>.
- [32] T. Xu, J. Flapper, Reduce energy use and greenhouse gas emissions from global dairy processing facilities, Energy Policy 39 (2011) 234–247, <https://doi.org/10.1016/j.enpol.2010.09.037>.
- [33] A. Banasik, J.M. Bloemhof-Ruwaard, A. Kanellopoulos, G.D.H. Claassen, J.G.A. J. van der Vorst, Multi-criteria decision making approaches for green supply chains: a review, Flexible Services and Manufacturing Journal 30 (2018) 366–396, <https://doi.org/10.1007/s10696-016-9263-5>.
- [34] P.M. Tomasula, N. Datta, W.C.F. Yee, A.J. McAloon, D.W. Nutter, F. Sampedro, L. M. Bonnaillie, Computer simulation of energy use, greenhouse gas emissions, and costs for alternative methods of processing fluid milk1, Journal of Dairy Science. 97 (2014) 4594–4611, <https://doi.org/10.3168/jds.2013-7546>.
- [35] P.M. Tomasula, W.C. Yee, A.J. McAloon, D.W. Nutter, L.M. Bonnaillie, Computer simulation of energy use, greenhouse gas emissions, and process economics of the fluid milk process, accessed April 5, 2023, Journal of Dairy Science (2013), [https://www.journalofdairyscience.org/article/S0022-0302\(13\)00225-7/fulltext](https://www.journalofdairyscience.org/article/S0022-0302(13)00225-7/fulltext).
- [36] J. Jouzdani, K. Govindan, On the sustainable perishable food supply chain network design: A dairy products case to achieve sustainable development goals, Journal of Cleaner Production. 278 (2021), 123060, <https://doi.org/10.1016/j.jclepro.2020.123060>.
- [37] E.G. Kirilova, N.G. Vakilieva-Bancheva, Environmentally friendly management of dairy supply chain for designing a green products' portfolio, Journal of Cleaner Production. 167 (2017) 493–504, <https://doi.org/10.1016/j.jclepro.2017.08.188>.
- [38] S.I. aan den Toorn, E. Worrell, M.A. van den Broek, Meat, dairy, and more: Analysis of material, energy, and greenhouse gas flows of the meat and dairy supply chains in the EU28 for 2016, Journal of Industrial Ecology. 24 (3) (2020) 601–614.
- [39] E. Frenette, O. Bahn, K. Vaillancourt, Meat, Dairy and Climate Change: Assessing the Long-Term Mitigation Potential of Alternative Agri-Food Consumption Patterns in Canada, Environmental Modeling and Assessment 22 (2017) 1–16, <https://doi.org/10.1007/s10666-016-9522-6>.
- [40] J. Upton, M. Murphy, L. Shalloo, P.W.G.G. Koerkamp, I.J.M.D. Boer, A mechanistic model for electricity consumption on dairy farms: Definition, validation, and demonstration, Journal of Dairy Science. 97 (2014) 4973–4984, <https://doi.org/10.3168/jds.2014-8015>.

- [41] M.S. Söylemez, Optimum heat pump in milk pasteurizing for dairy, *Journal of Food Engineering*. 74 (2006) 546–551, <https://doi.org/10.1016/j.jfoodeng.2005.01.046>.
- [42] G. Bylund, Dairy Processing Handbook, Dairy Processing Handbook. (1995). [https://dairyprocessinghandbook.tetrapak.com/\(accessed April 5, 2023\)](https://dairyprocessinghandbook.tetrapak.com/(accessed April 5, 2023)).
- [43] G. Singh, V.V. Tyagi, P.J. Singh, A.K. Pandey, Estimation of thermodynamic characteristics for comprehensive dairy food processing plant: An energetic and exergetic approach, *Energy* 194 (2020), 116799, <https://doi.org/10.1016/j.energy.2019.116799>.
- [44] R. Sinnott, G. Towler, Chemical engineering design: principles, practice and economics of plant and process design, Third edition, Butterworth-Heinemann, Oxford [England], 2022.
- [45] D.M. Himmelblau, J.B. Riggs, Basic principles and calculations in chemical engineering, 8th ed, Prentice Hall, Upper Saddle River, NJ, 2012.
- [46] M.C. Georgiadis, G.E. Rotstein, S. Macchietto, Modelling and simulation of complex plate heat exchanger arrangements under milk fouling, *Computers & Chemical Engineering*. 22 (1998) S331–S338, [https://doi.org/10.1016/S0098-1354\(98\)00072-6](https://doi.org/10.1016/S0098-1354(98)00072-6).
- [47] R. Sinnott, G. Towler, Chemical engineering design, 6th ed., Elsevier, Waltham, MA, 2019 [https://app.knovel.com/web/view/khtml/show.v/rcid:kpCEDE0001/cid:kt012GO1S1/viewerType:khtml/root\\_slug:chemical-engineering/url\\_slug:gasketed-plate-heat-exchangers?page=107&view=collapsed&zoom=1](https://app.knovel.com/web/view/khtml/show.v/rcid:kpCEDE0001/cid:kt012GO1S1/viewerType:khtml/root_slug:chemical-engineering/url_slug:gasketed-plate-heat-exchangers?page=107&view=collapsed&zoom=1).
- [48] J. Ahmed, M. Shafiur Rahman (Eds.), Handbook of Food Process Design, Wiley-Blackwell, Chichester, 2012.
- [49] R.P.M.A. Mehrabian, G.L. Quarini, Hydrodynamic and Thermal Characteristics of Corrugated Channels: Experimental Approach, *Experimental Heat Transfer*. 13 (2000) 223–234, <https://doi.org/10.1080/08916150050174904>.
- [50] R.W. Whitesides, Selecting the Optimum Pipe Size (2008).
- [51] PipeFlow Calculations, [www.Pipeflowcalculations.Com](http://www.Pipeflowcalculations.Com). (2020). <https://www.pipeflowcalculations.com/tables/stainless-schedule-40.xhtml> (accessed January 3, 2023).
- [52] D.I. Wilson, Fouling during food processing – progress in tackling this inconvenient truth, *Current Opinion in Food Science* 23 (2018) 105–112, <https://doi.org/10.1016/j.cofs.2018.10.002>.
- [53] T.K. Tuoc, Chapter 20 - Fouling in Dairy Processes, in: Z. Amjad, K.D. Demadis (Eds.), Mineral Scales and Deposits, Elsevier, Amsterdam, 2015, pp. 533–556, <https://doi.org/10.1016/B978-0-444-63228-9.00020-6>.
- [54] B. Bansal, X.D. Chen, A Critical Review of Milk Fouling in Heat Exchangers, *Comprehensive Reviews in Food Science and Food Safety*. 5 (2006) 27–33, <https://doi.org/10.1111/j.1541-4337.2006.tb00080.x>.
- [55] J.D. Brooks, S.H. Flint, Biofilms in the food industry: problems and potential solutions, *International Journal of Food Science & Technology*. 43 (2008) 2163–2176, <https://doi.org/10.1111/j.1365-2621.2008.01839.x>.
- [56] P.J. Fryer, K. Asteriadou, A prototype cleaning map: A classification of industrial cleaning processes, *Trends in Food Science & Technology*. 20 (2009) 255–262, <https://doi.org/10.1016/j.tifs.2009.03.005>.
- [57] S. Chandrakash. A new risk analysis of clean-in-place (CIP) milk processing., Thesis, 2012. <https://digital.library.adelaide.edu.au/dspace/handle/2440/76140> (accessed April 13, 2023).
- [58] M. Binama, A. Muhirwa, E. Bisengimana, Cavitation Effects in Centrifugal Pumps-A Review 6 (2016).
- [59] S. Gusew, R. Stuke, Pressure Drop in Plate Heat Exchangers for Single-Phase Convection in Turbulent Flow Regime: Experiment and Theory, *International Journal of Chemical Engineering*. 2019 (2019) e3693657. <https://doi.org/10.1155/2019/3693657>.
- [60] V. da S. Rosa, D. de M. Júnior, V. da S. Rosa, D. de M. Júnior, Design of Heat Transfer Surfaces in Agitated Vessels, *IntechOpen*, 2017. <https://doi.org/10.5772/66729>.
- [61] J. Kumana, S. Kathari, Predict storage tank heat transfer precisely, *Chemical Engineering (New York)*. 89 (1982) 127–132.
- [62] P. Brito, P. Lopes, P. Reis, O. Alves, Simulation and optimization of energy consumption in cold storage chambers from the horticultural industry, *International Journal of Energy and Environmental Engineering* 5 (2014) 88, <https://doi.org/10.1007/s40095-014-0088-2>.
- [63] H. Song, M. Cai, J. Cen, C. Xu, Q. Zeng, Research on energy saving optimization method of electric refrigerated truck based on genetic algorithm, *International Journal of Refrigeration*. 137 (2022) 62–69, <https://doi.org/10.1016/j.ijrefrig.2022.02.003>.
- [64] A.K. Coker, 5 - PUMPING OF LIQUIDS, in: A.K. Coker (Ed.), Ludwig's Applied Process Design for Chemical and Petrochemical Plants, (Fourth Edition), Gulf Professional Publishing, Burlington, 2007, pp. 303–369, <https://doi.org/10.1016/B978-075067766-0/50012-9>.
- [65] Chemical & Process Technology: Estimate Pump Power Consumption without Vendor Information, (n.d.). <http://webwormcpt.blogspot.com/2008/07/estimate-pump-power-consumption-without.html> (accessed April 5, 2023).
- [66] A. Chapman, K. Itakura, K. Hirose, F.T. Davidson, K. Nagasawa, A.C. Lloyd, M. E. Webber, Z. Kurban, S. Managi, T. Tamaki, M.C. Lewis, R.E. Hebner, Y. Fujii, A review of four case studies assessing the potential for hydrogen penetration of the future energy system, *International Journal of Hydrogen Energy*. 44 (2019) 6371–6382, <https://doi.org/10.1016/j.ijhydene.2019.01.168>.
- [67] Lj Energy Pte Ltd, Assessment Framework for Energy Efficiency Benchmarking Study of Food Manufacturing Plants, Lj Energy Pte Ltd, Singapore, 2015. <https://www.nea.gov.sg/docs/default-source/our-services/energy-efficiency/assessment-framework-for-fmbs.pdf> (accessed June 14, 2021).
- [68] S. Szepešs, P. Thorwid, Low Energy Consumption of High-Speed Centrifuges, *Chemical Engineering & Technology*. 41 (2018) 2375–2384, <https://doi.org/10.1002/ceat.201800292>.
- [69] M. Bertolini, E. Bottani, G. Vignali, A. Volpi, Comparative Life Cycle Assessment of Packaging Systems for Extended Shelf Life Milk, *Packaging Technology and Science*. 29 (2016) 525–546, <https://doi.org/10.1002/pts.2235>.
- [70] Y.-S. Lai, K.-Y. Lee, J.-H. Tseng, Y.-C. Chen, T.-L. Hsiao, Efficiency Comparison of PWM-Controlled and PAM-Controlled Sensorless BLDCM Drives for Refrigerator Applications, in: IEEE Industry Applications Annual Meeting 2007 (2007) 268–273, <https://doi.org/10.1109/07IAS.2007.5>.
- [71] S.A. Tassou, G. De-Lille, Y.T. Ge, Food transport refrigeration – Approaches to reduce energy consumption and environmental impacts of road transport, *Applied Thermal Engineering*. 29 (2009) 1467–1477, <https://doi.org/10.1016/j.applthermaleng.2008.06.027>.
- [72] S. Sato, Y.J. Jiang, R.L. Russell, J.W. Miller, G. Karavalakis, T.D. Durbin, K. C. Johnson, Experimental driving performance evaluation of battery-powered medium and heavy duty all-electric vehicles, *International Journal of Electrical Power & Energy Systems*. 141 (2022), 108100, <https://doi.org/10.1016/j.ijepes.2022.108100>.
- [73] S.A. Tassou, G. De-Lille, J. Lewis, Food transport refrigeration, Centre for Energy and Built Environment Research, Brunel University, UK, 2012. <https://www.grimsby.ac.uk/documents/defra/trms-refrigerenergy.pdf>.
- [74] U.S. Drive, Electrical and Electronics Technical Team Roadmap, U.S. Drive, 2017. <https://www.energy.gov/eere/vehicles/articles/us-drive-electrical-and-electronics-technical-team-roadmap>.
- [75] Digest of UK Energy Statistics (DUKES): calorific values and density of fuels, GOV. UK. (2022). <https://www.gov.uk/government/statistics/dukes-calorific-values> (accessed April 5, 2023).
- [76] Engineering toolbox, [www.Engineeringtoolbox.Com](http://www.Engineeringtoolbox.Com). (2023). [https://www.engineeringtoolbox.com/fuels-higher-calorific-values-d\\_169.html](https://www.engineeringtoolbox.com/fuels-higher-calorific-values-d_169.html) (accessed February 6, 2023).
- [77] Green Book, Data tables 1 to 19: supporting the toolkit and the guidance. Table 1: Electricity emissions factors to 2100, kgCO<sub>2</sub>e/kWh. Consumption and generation-based emissions. This set of tables supports the Treasury Green Book supplementary appraisal guidance on valuing energy use and greenhouse gas (GHG) emissions., (2019). [https://assets.publishing.service.gov.uk/government/uploads/system/uploads/attachment\\_data/file/793632/data-tables-1-19.xlsx](https://assets.publishing.service.gov.uk/government/uploads/system/uploads/attachment_data/file/793632/data-tables-1-19.xlsx) (accessed June 14, 2021).
- [78] K. de Kleijne, H. de Coninck, R. van Zelm, M.A.J. Huijbregts, S.V. Hanssen, The many greenhouse gas footprints of green hydrogen, *Sustainable Energy & Fuels*. 6 (2022) 4383–4387, <https://doi.org/10.1039/D2SE00444E>.
- [79] GOV UK, 2022 Government Greenhouse Gas Conversion Factors for Company Reporting - Methodology Paper for Conversion factors Draft Report, Department for Business, Energy, & Industrial Strategy, 2022. [https://assets.publishing.service.gov.uk/government/uploads/system/uploads/attachment\\_data/file/1083857/2022-ghg-cf-methodology-paper.pdf](https://assets.publishing.service.gov.uk/government/uploads/system/uploads/attachment_data/file/1083857/2022-ghg-cf-methodology-paper.pdf).
- [80] GOV UK, UK Low Carbon Hydrogen Standard - Guidance on the greenhouse gas emissions and sustainability criteria, 2022. <https://webarchive.nationalarchives.gov.uk/ukgwa/20230330002113/https://www.gov.uk/government/publications/uk-low-carbon-hydrogen-standard-emissions-reporting-and-sustainability-criteria>.
- [81] FDF, Decarbonisation of heat across the food and drink manufacturing sector, Food & Drink Federation (2021). <https://www.fdf.org.uk/globalassets/resources/publications/fdf-slr-report-decarbonising-heat-to-net-zero.pdf>.
- [82] T.C. Bond, B. Wehner, A. Plewka, A. Wiedensohler, J. Heintzenberg, R.J. Charlson, Climate-relevant properties of primary particulate emissions from oil and natural gas combustion, *Atmospheric Environment*. 40 (2006) 3574–3587, <https://doi.org/10.1016/j.atmosenv.2005.12.030>.
- [83] Appg. The role of hydrogen in powering industry, All Party Parliament Group, 2020.
- [84] A. Flysjö, M. Thrane, J.E. Hermansen, Method to assess the carbon footprint at product level in the dairy industry, *International Dairy Journal*. 34 (2014) 86–92, <https://doi.org/10.1016/j.idairyj.2013.07.016>.
- [85] A. M. Flysjö, Greenhouse gas emissions in milk and dairy product chains: Improving the carbon footprint of dairy products, (2012). <https://www.osti.gov/etdweb/biblio/22000600> (accessed April 15, 2023).
- [86] B. Coluccia, G.P. Agnusdei, F. De Leo, Y. Vecchio, C.M. La Fata, P.P. Miglietta, Assessing the carbon footprint across the supply chain: Cow milk vs soy drink, *The Science of the Total Environment* 806 (2022), 151200, <https://doi.org/10.1016/j.scitotenv.2021.151200>.